Inorg. Chem. **2007**, *46*, 10174–10186

Simultaneous Fluoride Binding to Ferrocene-Based Heteronuclear Bidentate Lewis Acids

Ramez Boshra, Krishnan Venkatasubbaiah, Ami Doshi, Roger A. Lalancette, Lazaros Kakalis, and Frieder Jäkle*

Department of Chemistry, Rutgers University, Newark, 73 Warren Street, Newark, New Jersey 07102

Received July 10, 2007

A series of μ_2-fluoro-bridged heteronuclear bidentate Lewis acid complexes [K(18-crown-6)THF]$^+$ [Fc(BMeF)($SnMe_2Cl$)F]$^-$ **(1-2F)**, [K(18-crown-6)THF]$^+$ [Fc(BMeF)($SnMe_2F$)F]$^-$ **(1-3F)**, [K(18-crown-6)THF]$^+$ [Fc(BMePh)($SnMe_2Cl$)F]$^-$ **(2-F)**, and [K(18-crown-6)THF]$^+$ [Fc(BMePh)($SnMe_2F$)F]$^-$ **(2-2F)** (Fc = 1,2-ferrocenediyl) was prepared. Compounds **2-F** and **2-2F** were obtained as a mixture of diastereomers, which arise due to the generation of a stereocenter at boron in addition to their inherent planar chirality. All compounds have been studied in the solid state by single-crystal X-ray diffraction analysis and by multinuclear NMR spectroscopy in solution. As a result of bridging-fluoride interactions, tetrahedral boron and distorted trigonal-bipyramidal tin centers are observed. Comparison with the corresponding monofunctional ferrocenylborates further supports the bridging nature of the fluoride anion. Two-dimensional exchange spectroscopy ^{19}F NMR studies provide evidence for facile intermolecular and intramolecular fluorine exchange processes. All complexes display reversible one-electron oxidation events at lower potentials than those of the tricoordinate ferrocenylborane precursors, which is typical of ferrocenylborate complexes.

Introduction

Bi- and multidentate Lewis acids represent an interesting class of Lewis acids that has seen a growing interest in recent years.[1−3] Since their first preparation more than four decades ago, bidentate Lewis acids have been recognized for their unique ability to form reverse chelates,[4−7] superior performance in catalysis when compared with the respective monofunctional Lewis acids,[2,8] and their suitability as building blocks for the preparation of new materials.[9] Recently, bi- and multidentate Lewis acids have assumed important roles in anion recognition,[10] particularly as fluoride-sensing materials.[11−14] For instance, Gabbaï and co-workers devised an intriguing organoboron bidentate Lewis acid system (**A**[13,15]) capable of fluoride complexation with binding constants that are several orders of magnitude higher than those of the monodentate Lewis acid counterparts.[16,17]

* To whom correspondence should be addressed. E-mail: fjaekle@rutgers.edu.

(1) (a) Vaugeois, J.; Simard, M.; Wuest, J. D. *Coord. Chem. Rev.* **1995**, *145*, 55−73. (b) Jäkle, F. In *Group 13 Chemistry: From Fundamentals to Applications*; ACS Symposium Series 822; American Chemical Society: Washington, DC, 2002; pp 104−117. (c) Gabbaï, F. P. *Angew. Chem., Int. Ed.* **2003**, *42*, 2218−2221. (d) Dembitsky, V. M.; Abu Ali, H.; Srebnik, M. *Appl. Organomet. Chem.* **2003**, *17*, 327−345. (e) Wedge, T. J.; Hawthorne, M. F. *Coord. Chem. Rev.* **2003**, *240*, 111−128. (f) Melaïmi, M.; Gabbaï, F. P. *Adv. Organomet. Chem.* **2005**, *53*, 61−99.

(2) Piers, W. E.; Irvine, G. J.; Williams, V. C. *Eur. J. Inorg. Chem.* **2000**, 2131−2142.

(3) Hoefelmeyer, J. D.; Schulte, M.; Tschinkl, M.; Gabbaï, F. P. *Coord. Chem. Rev.* **2002**, *235*, 93−103.

(4) Shriver, D. F.; Biallas, M. J. *J. Am. Chem. Soc.* **1967**, *89*, 1078−1081.

(5) (a) Katz, H. E. *J. Am. Chem. Soc.* **1985**, *107*, 1420−1421. (b) Blanda, M. T.; Horner, J. H.; Newcomb, M. *J. Org. Chem.* **1989**, *54*, 4626−4636. (c) Köster, R.; Seidel, G.; Wagner, K.; Wrackmeyer, B. *Chem. Ber.* **1993**, *126*, 305−317. (d) Tamao, K.; Hayashi, T.; Ito, Y. *J. Organomet. Chem.* **1996**, *506*, 85−91. (e) Vaugeois, J.; Wuest, J. D. *J. Am. Chem. Soc.* **1998**, *120*, 13016−13022. (f) Uhl, W.; Hannemann, F. *J. Organomet. Chem.* **1999**, *579*, 18−23. (g) Lopez, P.; Oh, T. *Tetrahedron Lett.* **2000**, *41*, 2313−2317. (h) Tschinkl, M.; Bachman, R. E.; Gabbaï, F. P. *Organometallics* **2000**, *19*, 2633−2636. (i) Ghesner, I.; Piers, W. E.; Parvez, M.; McDonald, R. *Organometallics* **2004**, *23*, 3085−3087.

(6) Altmann, R.; Jurkschat, K.; Schurmann, M.; Dakternieks, D.; Duthie, A. *Organometallics* **1998**, *17*, 5858−5866.

(7) Venkatasubbaiah, K.; Bats, J. W.; Rheingold, A. L.; Jäkle, F. *Organometallics* **2005**, *24*, 6043−6050.

(8) (a) Chen, E. Y.-X.; Marks, T. J. *Chem. Rev.* **2000**, *100*, 1391−1434. (b) Pédeutour, J.-N.; Radhakrishnan, K.; Cramail, H.; Deffieux, A. *Macromol. Rapid Comm.* **2001**, *22*, 1095−1123. (c) Williams, V. C.; Irvine, G. J.; Piers, W. E.; Li, Z. M.; Collins, S.; Clegg, W.; Elsegood, M. R. J.; Marder, T. B. *Organometallics* **2000**, *19*, 1619−1621. (d) Oh, T.; Lopez, P.; Reilly, M. *Eur. J. Org. Chem.* **2000**, *16*, 2901−2903. (e) Lewis, S. P.; Henderson, L. D.; Chandler, B. D.; Parvez, M.; Piers, W. E.; Collins, S. *J. Am. Chem. Soc.* **2003**, *125*, 14686−14687. (f) King, J. B.; Gabbaï, F. P. *Organometallics* **2003**, *22*, 1275−1280. (g) Ooi, T.; Takahashi, M.; Yamada, M.; Tayama, E.; Omoto, K.; Maruoka, K. *J. Am. Chem. Soc.* **2004**, *126*, 1150−1160.

10.1021/ic7013754 CCC: $37.00
Published on Web 11/03/2007

Remarkably, Jurkschat and co-workers have reported a series of organotin-based bidentate Lewis acids (e.g., **B**[6]) that cooperatively bind to various nucleophiles and, in some cases, show a strong preference for fluoride binding.[11,18,19] However, simultaneous fluoride binding to boron and tin centers in reverse chelates has not been reported to date, although interaction of a BF_4^- fluorine atom with cationic organotin moieties has been found[20] and a number of potentially suitable heteronuclear Sn/B receptors have been described.[21]

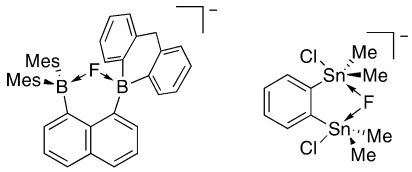

A **B**

In addition to the strength of the Lewis acid centers involved in the complexation process, the affinity toward nucleophiles is greatly influenced by the structure of the host molecule. In general, the entropy change of flexible bidentate Lewis acid systems does not favor the cooperative binding effect.[3,4,22] Hence, the pre-organization of the Lewis acidic sites of the host molecule is of great importance to the stability of the "host−guest" complexes, and typically the selectivity also improves with more rigid structures. For instance, *o*-phenylene ditin,[6] *o*-phenylene dimercury,[23] and *o*-phenylene or 1,8-naphthalene diboron[3,24] Lewis acids display a strong tendency for simultaneous binding of nucleophiles.

Among different architectures of polyfunctional Lewis acids with a rigid backbone, 1,2-disubstituted ferrocene-based Lewis acids have attracted our particular interest.[7,25−28] Their three-dimensional structure, inherent planar chirality in the case of systems with two different Lewis acid sites (heteronuclear bidentate Lewis acids), and redox activity distinguish them from other bidentate Lewis acids.[12,29,30] We have

(9) (a) Gabbaï, F. P.; Schier, A.; Riede, J. *Angew. Chem., Int. Ed.* **1998**, *37*, 622−624. (b) Gardinier, J. R.; Gabbaï, F. P. *J. Chem. Soc., Dalton Trans.* **2000**, 2861−2865. (c) Ding, L.; Ma, K. B.; Durner, G.; Bolte, M.; de Biani, F. F.; Zanello, P.; Wagner, M. *J. Chem. Soc., Dalton Trans.* **2002**, 1566−1573. (d) Ma, K.; Scheibitz, M.; Scholz, S.; Wagner, M. *J. Organomet. Chem.* **2002**, *652*, 11−19. (e) Heilmann, J. B.; Scheibitz, M.; Qin, Y.; Sundararaman, A.; Jäkle, F.; Kretz, T.; Bolte, M.; Lerner, H.-W.; Holthausen, M. C.; Wagner, M. *Angew. Chem., Int. Ed.* **2006**, *45*, 920−925.

(10) (a) Schmidtchen, F. P.; Berger, M. *Chem. Rev.* **1997**, *97*, 1609−1646. (b) Antonisse, M. M. G.; Reinhoudt, D. N. *Chem. Commun.* **1998**, 443−448. (c) Beer, P. D.; Gale, P. A. *Angew. Chem., Int. Ed.* **2001**, *40*, 486−516.

(11) (a) Perdikaki, K.; Tsagatakis, I.; Chaniotakis, N. A.; Altmann, R.; Jurkschat, K.; Reeske, G. *Anal. Chim. Acta* **2002**, *467*, 197−204. (b) Chaniotakis, N.; Jurkschat, K.; Müller, D.; Perdikaki, K.; Reeske, G. *Eur. J. Inorg. Chem.* **2004**, 2283−2288.

(12) Bresner, C.; Day, J. K.; Coombs, N. D.; Fallis, I. A.; Aldridge, S.; Coles, S. J.; Hursthouse, M. B. *Dalton Trans.* **2006**, 3660−3667.

(13) Melaïmi, M.; Solé, S.; Chiu, C. W.; Wang, H.; Gabbaï, F. P. *Inorg. Chem.* **2006**, *45*, 8136−8143.

(14) (a) Miyata, M.; Chujo, Y. *Polym. J.* **2002**, *34*, 967−969. (b) Parab, K.; Venkatasubbaiah, K.; Jäkle, F. *J. Am. Chem. Soc.* **2006**, *128*, 12879−12885.

(15) Solé, S.; Gabbaï, F. P. *Chem. Commun.* **2004**, 1284−1285.

(16) Heteronuclear bidentate Lewis acids and systems that contain boron moieties and ammonium or phosphonium cation centers have also been reported: (a) Melaïmi, M.; Gabbaï, F. P. *J. Am. Chem. Soc.* **2005**, *127*, 9680−9681. (b) Chiu, C.-W.; Gabbaï, F. P. *J. Am. Chem. Soc.* **2006**, *128*, 14248−14249. (c) Agou, T.; Kobayashi, J.; Kawashima, T. *Inorg. Chem.* **2006**, *45*, 9137−9144. (d) Lee, M. H.; Agou, T.; Kobayashi, J.; Kawashima, T.; Gabbaï, F. P. *Chem. Commun.* **2007**, 1133−1135.

(17) For other recent examples of anion binding to organoboranes, see: (a) Yamaguchi, S.; Akiyama, S.; Tamao, K. *J. Am. Chem. Soc.* **2001**, *123*, 11372−11375. (b) Suri, J. T.; Cordes, D. B.; Cappuccio, F. E.; Wessling, R. A.; Singaram, B. *Angew. Chem., Int. Ed.* **2003**, *42*, 5857−5859. (c) Kubo, Y.; Yamamoto, M.; Ikeda, M.; Takeuchi, M.; Shinkai, S.; Yamaguchi, S.; Tamao, K. *Angew. Chem., Int. Ed.* **2003**, *42*, 2036−2040. (d) Zhu, L.; Zhong, Z.; Anslyn, E. V. *J. Am. Chem. Soc.* **2005**, *127*, 4260−4267. (e) Koskela, S. J. M.; Fyles, T. M.; James, T. D. *Chem. Commun.* **2005**, 945−947. (f) Kubo, Y.; Ishida, T.; Kobayashi, A.; James, T. D. *J. Mater. Chem.* **2005**, *15*, 2889−2895. (g) Liu, Z.-Q.; Shi, M.; Li, F.-Y.; Fang, Q.; Chen, Z.-H.; Yi, T.; Huang, C.-H. *Org. Lett.* **2005**, *7*, 5481−5484. (h) Neumann, T.; Dienes, Y.; Baumgartner, T. *Org. Lett.* **2006**, *8*, 495−497. (i) Sakuda, E.; Funahashi, A.; Kitamura, N. *Inorg. Chem.* **2006**, *45*, 10670−10677. (j) Liu, X. Y.; Bai, D. R.; Wang, S. *Angew. Chem., Int. Ed.* **2006**, *45*, 5475−5478. (k) Sun, Y.; Ross, N.; Zhao, S.-B.; Huszarik, K.; Jia, W.-L.; Wang, R.-Y.; Macartney, D.; Wang, S. *J. Am. Chem. Soc.* **2007**, *129*, 7510−7511.

(18) Dakternieks, D.; Jurkschat, K.; Zhu, H. J.; Tiekink, E. R. T. *Organometallics* **1995**, *14*, 2512−2521.

(19) Schulte, M.; Schurmann, M.; Jurkschat, K. *Chem.—Eur. J.* **2001**, *7*, 347−355.

(20) (a) Grützmacher, H.; Pritzkow, H. *Organometallics* **1991**, *10*, 938−946. (b) Blackwell, J. M.; Piers, W. E.; McDonald, R. *J. Am. Chem. Soc.* **2002**, *124*, 1295−1306.

(21) (a) Nöth, H.; Otto, P.; Storch, W. *Chem. Ber.* **1986**, *119*, 2517−2530. (b) Köster, R.; Seidel, G.; Boese, R.; Wrackmeyer, B. *Chem. Ber.* **1988**, *121*, 597−615. (c) Wrackmeyer, B.; Kerschl, S.; Maisel, H. E.; Milius, W. *J. Organomet. Chem.* **1995**, *490*, 197−202. (d) Eisch, J. J.; Kotowicz, B. W. *Eur. J. Inorg. Chem.* **1998**, 761−769. (e) Schulte, M.; Gabbaï, F. P. *Can. J. Chem.* **2002**, *80*, 1308−1312. (f) Wrackmeyer, B.; Kehr, G.; Willbold, S. *J. Organomet. Chem.* **1999**, *590*, 93−103.

(22) (a) Biallas, M. J. *J. Am. Chem. Soc.* **1969**, *91*, 7290−7292. (b) Biallas, M. J. *Inorg. Chem.* **1971**, *10*, 1320−1322.

(23) (a) Tschinkl, M.; Schier, A.; Riede, J.; Gabbaï, F. P. *Organometallics* **1999**, *18*, 1747−1753. (b) Beauchamp, A. L.; Olivier, M. J.; Wuest, J. D.; Zacharie, B. *J. Am. Chem. Soc.* **1986**, *108*, 73−77. (c) Beauchamp, A. L.; Olivier, M. J.; Wuest, J. D.; Zacharie, B. *Organometallics* **1987**, *6*, 153−156.

(24) (a) Lopez, P.; Oh, T. *Tetrahedron Lett.* **2000**, *41*, 2313−2317. (b) Chase, P. A.; Henderson, L. D.; Piers, W. E.; Parvez, M.; Clegg, W.; Elsegood, M. R. J. *Organometallics* **2006**, *25*, 349−357.

(25) Jäkle, F.; Lough, A. J.; Manners, I. *Chem. Commun.* **1999**, 453−454.

(26) Gamboa, J. A.; Sundararaman, A.; Kakalis, L.; Lough, A. J.; Jäkle, F. *Organometallics* **2002**, *21*, 4169−4181.

(27) Boshra, R.; Sundararaman, A.; Zakharov, L. N.; Incarvito, C. D.; Rheingold, A. L.; Jäkle, F. *Chem.—Eur. J.* **2005**, *11*, 2810−2824.

(28) (a) Venkatasubbaiah, K.; Zakharov, L. N.; Kassel, W. S.; Rheingold, A. L.; Jäkle, F. *Angew. Chem., Int. Ed.* **2005**, *44*, 5428−5433. (b) Venkatasubbaiah, K.; DiPasquale, A. G.; Bolte, M.; Rheingold, A. L.; Jäkle, F. *Angew. Chem., Int. Ed.* **2006**, *45*, 6838−6841. (c) Venkatasubbaiah, K.; Nowik, I.; Herber, R. H.; Jäkle, F. *Chem. Commun.* **2007**, 2154−2156.

(29) For metallocene-based bifunctional Lewis acids derived from 1,1′-disubstituted ferrocenes, see: (a) Grosche, M.; Herdtweck, E.; Peters, F.; Wagner, M. *Organometallics* **1999**, *18*, 4669−4672. (b) Herberhold, M.; Milius, W.; Steffl, U.; Vitzithum, K.; Wrackmeyer, B.; Herber, R. H.; Fontani, M.; Zanello, P. *Eur. J. Inorg. Chem.* **1999**, 145−151. (c) Altmann, R.; Gausset, O.; Horn, D.; Jurkschat, K.; Schurmann, M.; Fontani, M.; Zanello, P. *Organometallics* **2000**, *19*, 430−443. (d) Uhl, W.; Hahn, I.; Jantschak, A.; Spies, T. *J. Organomet. Chem.* **2001**, *637−639*, 300−303. (e) Carpenter, B. E.; Piers, W. E.; McDonald, R. *Can. J. Chem.* **2001**, *79*, 291−295. (f) Aldridge, S.; Bresner, C.; Fallis, I. A.; Coles, S. J.; Hursthouse, M. B. *Chem. Commun.* **2002**, 740−741. (g) Scheibitz, M.; Bolte, M.; Lerner, H. W.; Wagner, M. *Organometallics* **2004**, *23*, 3556−3559. (h) Braunschweig, H.; Burschka, C.; Clentsmith, G. K. B.; Kupfer, T.; Radacki, K. *Inorg. Chem.* **2005**, *44*, 4906−4908. (i) Bresner, C.; Aldridge, S.; Fallis, I. A.; Jones, C.; Ooi, L.-L. *Angew. Chem., Int. Ed.* **2005**, *44*, 3606−3609. (j) Althoff, A.; Eisner, D.; Jutzi, P.; Lenze, N.; Neumann, B.; Schoeller, W. W.; Stammler, H. G. *Chem.—Eur. J.* **2006**, *12*, 5471−5480.

(30) Herberich, G. E.; Englert, U.; Fischer, A.; Wiebelhaus, D. *Eur. J. Inorg. Chem.* **2004**, 4011−4020.

Scheme 1. Preparation of Reverse Chelates with Fluoride[a]

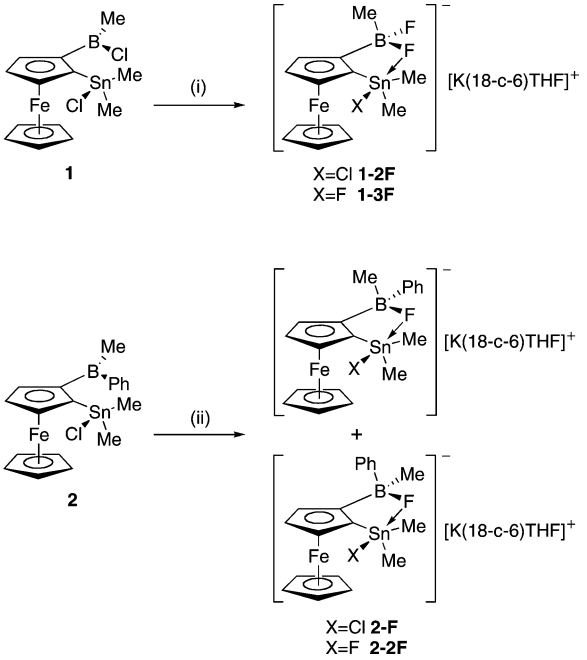

[a] Reagents and conditions: (i) For **1-2F**; 1.7 equiv KF, THF, 18-crown-6, r.t., 48 h. For **1-3F**; excess KF, THF, 18-crown-6, 50 °C, 48 h. (ii) For **2-F**; 1.0 equiv KF, THF, 18-crown-6, r.t., 48 h. For **2-2F**; excess KF, THF, 18-crown-6, 50 °C, 48 h.

previously shown that the heteronuclear bidentate ferrocene-based Lewis acids **1** and **2** that feature adjacent organotin and organoboron Lewis acid sites function in a cooperative fashion, as evident from their enhanced Lewis acidity compared with that of the monofunctional Lewis acids.[27] We have also demonstrated that the binding of pyridine proceeds in a regio- and stereoselective manner as a result of intramolecular interaction between the two Lewis acidic centers, which is promoted by the halide substituents on boron. In this work, we expanded our efforts to study the recognition of anions, particularly the binding of fluoride. Aided by the strong coupling of fluorine to various NMR-active nuclei and through X-ray diffraction studies, we have probed the precise nature of the anion binding process both in solution and in the solid state.

Results and Discussion

Synthetic Aspects. The synthesis of the heteronuclear bidentate Lewis acids **1** and **2** has been reported previously.[26] Treatment of **1** with 1.7 equiv KF in the presence of 18-crown-6 at room temperature afforded the fluoride complex **1-2F** in ca. 66% yield (Scheme 1). The use of excess KF in the presence of 18-crown-6 at 45−50 °C led to the exchange of the tin-bound chlorine for fluorine with the formation of **1-3F** in 65% yield. Similarly, the treatment of **2** with 1 equiv and excess KF gave the fluoride complexes **2-F** (71%) and **2-2F** (64%), respectively. To explore the consequences of having two adjacent Lewis acid centers on the fluoride binding, we also prepared the corresponding monofunctional organoboron Lewis acid complexes. The fluoride complexes **3-2F** and **4-F** were obtained in 58 and 51% yield, respectively, upon treatment of the Lewis acids **3**[27] and **4**[27] with

Scheme 2. Preparation of Fluoride Model Complexes[a]

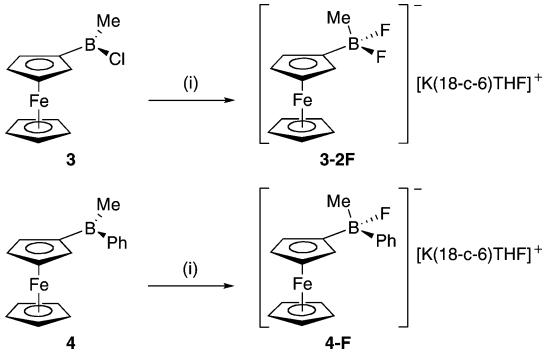

[a] Reagents and conditions: (i) Excess KF, THF, 18-crown-6, r.t., 48 h.

excess KF in the presence of 1 equiv of 18-crown-6 at room temperature (Scheme 2). The fluoride coordination can be visually observed by a color change from orange-red to yellow. Unlike the precursors, all compounds synthesized are air-stable in the solid state for extended periods of time. The structure of the new complexes was confirmed by multinuclear NMR spectroscopy, single-crystal X-ray diffraction, and elemental analysis.

Solid-State Structures. Single-crystal X-ray diffraction analyses of **1-2F**, **1-3F**, **2-F**, **2-2F**, and **4-F** were performed on light orange crystals obtained from a mixture of THF and ether at −37 °C. Crystals of **3-2F** were grown by the slow evaporation of a solution in CH_2Cl_2/hexanes. Their molecular structures are shown in Figures 1−3, and selected bond lengths and angles for the bidentate Lewis acid complexes are listed in Table 1. Two independent molecules with similar geometric parameters and a cocrystallized water molecule that was also confirmed by ^{1}H NMR spectroscopy were found in the unit cell for **3-2F**. One of the main molecules is shown in Figure 3, and the structure of the other molecule is displayed in Figure S1 in the Supporting Information.

General Characteristics. All bidentate Lewis acid complexes feature the fluorine atom in an unsymmetrical bridging position between the Lewis acidic boron and tin centers. The heavier chlorine atom in compounds **1-2F** and **2-F** occupies the terminal rather than the bridging position. This preference can be explained by invoking the hard−soft acid−base principle that predicts the binding of chloride to be more favorable to the larger (and softer) tin center.[18,31] The binding of fluoride to compound **2** results in formation of boron-chiral complexes[32] with four different substituents on boron (Figure 2). However, only one of the two possible diastereomers is observed in the solid-state structures of complexes **2-F** and **2-2F**. Interestingly, for complex **2-F**, the R_B, S_p and S_B, R_p enantiomer pair with a phenyl group that is positioned above the Cp plane crystallizes, while the R_B, R_p and S_B, S_p enantiomer pair is found for **2-2F** with the phenyl ring positioned close to the Fe center (the descriptors R_B and S_B

(31) Hoefelmeyer, J. D.; Gabbaï, F. P. *Chem. Commun.* **2003**, 712−713.
(32) (a) Vedejs, E.; Chapman, R. W.; Lin, S.; Müller, M.; Powell, D. R. *J. Am. Chem. Soc.* **2000**, *122*, 3047. (b) Burgos, C. H.; Canales, E.; Matos, K.; Soderquist, J. A. *J. Am. Chem. Soc.* **2005**, *127*, 8044−8049.

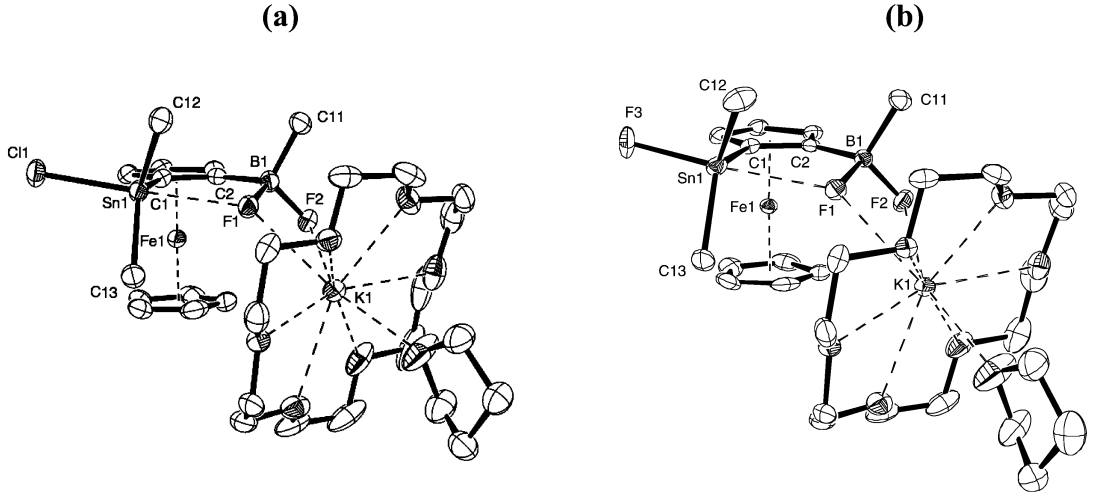

Figure 1. (a) Molecular structure of $[K(18\text{-crown-6})THF]^+$ $[Fc(BMeF)(SnMe_2Cl)F]^-$ **(1-2F)** (ORTEP, 50% probability). The THF molecule is disordered over two positions. (b) Molecular structure of $[K(18\text{-crown-6})THF]^+$ $[Fc(BMeF)(SnMe_2F)F]^-$ **(1-3F)** (ORTEP, 50% probability). Hydrogen atoms are omitted for clarity, and only one of the planar chiral enantiomers is shown.

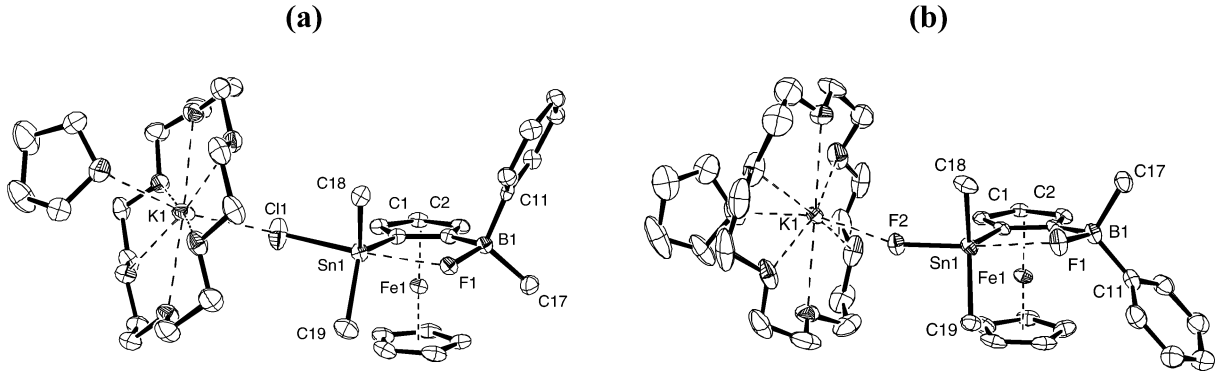

Figure 2. (a) Molecular structure of $[K(18\text{-crown-6})THF]^+$ $[Fc(BMePh)(SnMe_2Cl)F]^-$ **(2-F)** (ORTEP, 50% probability). (b) Molecular structure of $[K(18\text{-crown-6})THF]^+$ $[Fc(BMePh)(SnMe_2F)F]^-$ **(2-2F)** (ORTEP, 30% probability). Hydrogen atoms are omitted for clarity, and only one of the planar chiral enantiomers is shown.

refer to the central chirality at boron and R_p and S_p refer to the planar chirality). The monofunctional borate **4-F** forms a racemate and crystallizes in the achiral *P*2(1)/*c* space group with the phenyl ring pointing away from the ferrocene moiety (Figure 3).

Boron Environment. Coordination of the fluoride anion to boron results in elongation of the Cp−B (Cp = cyclopentadienyl) bond as a result of the change to the sp^3 hybridization on boron.[33,34] The Cp−B bond distances for **1-2F**, **1-3F**, **2-F**, and **2-2F** range from 1.605(4) to 1.619(10) Å and are thus significantly longer than those of the precursors **1** and **2**, which average 1.529 Å. Additionally, the bending of the boryl group toward iron, measured as 180° − Cp_{Cent}−C(2)−B(1), is less pronounced than that for the starting material or completely absent. For the free acids **1** and **2**, the relatively large bent angles of 13.8° and 12.2°, respectively, can be attributed to a delocalized interaction of the electron-rich iron center and the electron-deficient boron via the Cp ring, as recently shown by Wagner et al.[35]

For **1-2F** and **1-3F**, the bent angles toward Fe average 3.8°, and for the phenyl-substituted species **2-F** and **2-2F**, bent angles of 3.6° and 6.3° are realized, respectively, where the boryl groups point away from the iron center. The latter is likely a result of steric congestion upon the tetracoordination of boron and also observed for the monofunctional complex **4F** (180° − Cp_{Cent}−C(1)−B(1) = 3.3°).

Two fluorine atoms are attached to boron in **1-2F** and **1-3F**, one of which is in a bridging position (F_{br}) and pointing downward toward tin, while the other one is pointing downward but away from tin. The B−F distances for the fluorine atoms that point toward tin (**1-2F**, 1.500(3) Å; **1-3F**, 1.492(3) Å) are significantly longer than the terminal B−F distances (**1-2F**, 1.435(4) Å; **1-3F**, 1.443(3) Å) and also longer than the B−F distance for the monofunctional fluoroborate **3-2F** (average 1.451 Å). For complexes **2-F** and **2-2F**, B−F distances of 1.530(3) and 1.530(9) Å, respectively, are observed. Again a distinct impact of the adjacent tin center is evident from comparison with the B−F bond distance in the monofunctional complex **4-F** (1.474(3) Å). The even longer distances in comparison to **1-2F** and **1-3F** may be attributed at least in part to the lower Lewis acidity

(33) Aldridge, S.; Bresner, C. *Coord. Chem. Rev.* **2003**, *244*, 71−92.
(34) Scheibitz, M.; Heilmann, J. B.; Winter, R. F.; Bolte, M.; Bats, J. W.; Wagner, M. *Dalton Trans.* **2005**, 159−170.
(35) Scheibitz, M.; Bolte, M.; Bats, J. W.; Lerner, H.-W.; Nowik, I.; Herber, R. H.; Krapp, A.; Lein, M.; Holthausen, M.; Wagner, M. *Chem.—Eur. J.* **2005**, *11*, 584−603.

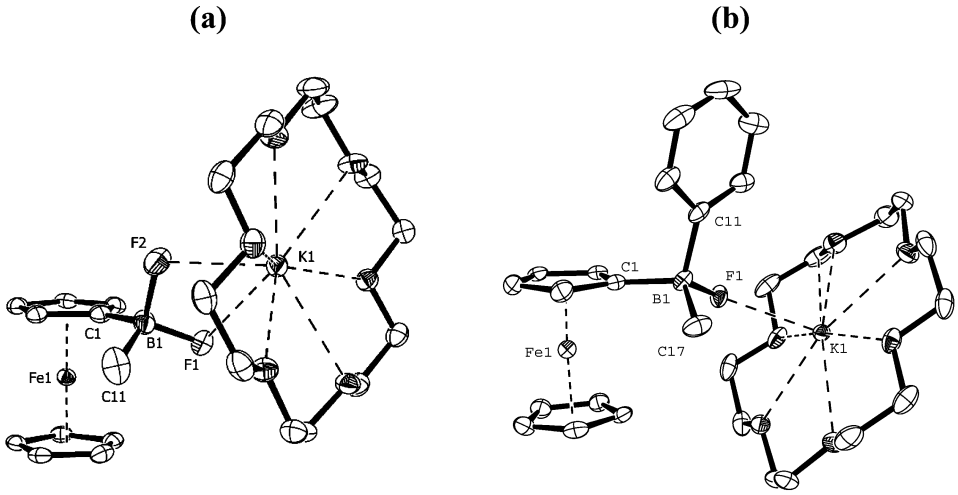

Figure 3. (a) Molecular structure of one of the two independent molecules of $[K(18\text{-crown-6})]^+$ $[Fc(BMeF)F]^-$ **(3-2F)** (ORTEP, 50% probability). Hydrogens and a cocrystallized water molecule are omitted for clarity. Selected bond lengths (Å) and angles (deg): B(1)−C(1) 1.622(4), B(1)−C(11) 1.606(5), B(1)−F(1) 1.433(3), B(1)−F(2) 1.464(3), F(1)−K(1) 2.8931(17), F(2)−K(1) 2.6449(18), F(1)−B(1)−C(1) 110.2(2), F(1)−B(1)−C(11) 111.8(2), F(2)−B(1)−C(11) 108.1(3), F(2)−B(1)−C(1) 108.5(2), F(1)−B(1)−F(2) 103.8(2), C(1)−B(1)−C(11) 113.9(2), B(1)−F(1)−K(1) 94.97(14), B(1)−F(2)−K(1) 105.22(15). (b) Molecular structure of $[K(18\text{-crown-6})]^+$ $[Fc(BMePh)F]^-$ **(4-F)** (ORTEP, 50% probability). Hydrogens are omitted for clarity. Selected bond length (Å) and angles (deg): B(1)−C(1) 1.629(4), B(1)−C(11) 1.631(4), B(1)−C(17) 1.630(4), B(1)−F(1) 1.474(3), K(1)−F(1) 2.5695(16), F(1)−B(1)−C(1) 107.5-(2), F(1)−B(1)−C(11) 107.4(2), F(1)−B(1)−C(17) 108.7(2), C(1)−B(1)−C(11) 108.0(2), C(1)−B(1)−C(17) 113.2(2), C(11)−B(1)−C(17) 111.8(2), B(1)−F(1)−K(1) 130.13(15).

Table 1. Selected Bond Lengths (Å), Interatomic Distances (Å), and Angles (deg) for **1-2F**, **1-3F**, **2-F**, and **2-2F**

	1-2F	**1-3F**		**2-F**	**2-2F**
Sn(1)−Cl(1)/F(3)	2.4313(6)	2.0095(13)	Sn(1)−Cl(1)/F(2)	2.4346(9)	2.013(4)
Sn(1)−C(1)	2.099(2)	2.096(2)	Sn(1)−C(1)	2.101(3)	2.082(6)
Sn(1)−C(12)	2.132(3)	2.121(2)	Sn(1)−C(18)	2.126(3)	2.123(7)
Sn(1)−C(13)	2.127(3)	2.127(2)	Sn(1)−C(19)	2.120(3)	2.116(6)
B(1)−C(2)	1.615(4)	1.609(3)	B(1)−C(2)	1.605(4)	1.619(10)
B(1)−C(11)	1.608(4)	1.606(3)	B(1)−C(17)	1.613(4)	1.632(10)
B(1)−F(2)	1.435(4)	1.443(3)	B(1)−C(11)	1.634(4)	1.609(11)
B(1)−F(1)	1.500(3)	1.492(3)	B(1)−F(1)	1.530(3)	1.530(9)
Fe(1)···B(1)	3.285	3.265	Fe(1)···B(1)	3.355	3.394
Sn(1)···F(1)	2.588(2)	2.642(1)	Sn(1)···F(1)	2.420(2)	2.379(4)
C(1)−Sn(1)−C(13)	123.05(11)	122.03(11)	C(1)−Sn(1)−C(19)	122.11(12)	120.3(3)
C(1)−Sn(1)−C(12)	115.43(10)	116.08(11)	C(1)−Sn(1)−C(18)	118.19(11)	113.6(2)
C(12)−Sn(1)−C(13)	115.01(11)	114.72(12)	C(18)−Sn(1)−C(19)	114.99(13)	120.4(3)
C(13)−Sn(1)−Cl(1)/F(3)	98.73(8)	99.01(9)	C(19)−Sn(1)−Cl(1)/F(2)	98.82(10)	97.5(2)
C(1)−Sn(1)−Cl(1)/F(3)	96.06(7)	97.53(7)	C(1)−Sn(1)−Cl(1)/F(2)	95.45(8)	99.9(2)
C(12)−Sn(1)−Cl(1)/F(3)	100.98(8)	100.60(10)	C(18)−Sn(1)−Cl(1)/F(2)	97.54(8)	96.4(3)
F(1)−Sn(1)−Cl(1)/F(3)	169.66(3)	170.49(5)	F(1)−Sn(1)−Cl(1)/F(2)	171.11(4)	175.21(15)
C(2)−B(1)−C(11)	115.4(2)	115.68(18)	C(2)−B(1)−C(11)	111.2(2)	118.1(6)
C(2)−B(1)−F(2)	112.1(2)	111.75(17)	C(2)−B(1)−C(17)	116.3(3)	110.8(6)
C(11)−B(1)−F(2)	110.4(2)	109.45(18)	C(11)−B(1)−C(17)	110.0(2)	110.4(6)
F(1)−B(1)−F(2)	104.4(2)	104.76(18)	C(2)−B(1)−F(1)	103.6(2)	104.5(5)
F(1)−B(1)−C(2)	105.27(19)	105.23(18)	C(17)−B(1)−F(1)	108.1(2)	105.9(6)
C(11)−B1−C(2)	115.4(2)	115.41(19)	C(11)−B1−F(1)	107.0(2)	106.1(6)
Cp staggering angle	35.6	32.6	Cp staggering angle	17.6	12.6
180 − Cp_{Cent}−C(2)−B(1)[a]	3.9 (dn)	3.7 (dn)	180 − Cp_{Cent}−C(2)−B(1)[a]	3.6 (up)	6.3 (up)
180 − Cp_{Cent}−C(1)−Sn(1)[a]	4.0 (dn)	3.6 (dn)	180 − Cp_{Cent}−C(1)−Sn(1)[a]	5.7 (dn)	6.4 (dn)

[a] The position of the boryl group relative to the Cp ring is indicated as "dn" for bending toward Fe and as "up" for bending away from Fe; Cp_{Cent} refers to the centroid of the substituted Cp ring.

of the boron centers in the presence of a phenyl substituent as opposed to an additional fluoride ligand in **1-2F** and **1-3F**.

The tetrahedral character at boron has been defined in the literature as % THC = $[(120° - X)/(120° - 109.5°)] \times 100\%$, where X is the average angle between the three boron substituents already present in the free acid.[36] The values calculated for % THC range from 70.2% (**1-2F**) to 73.4% (**1-3F**) for the fluoride complexes of the bidentate Lewis acid complexes. This stands in sharp contrast to an estimated 84 and 86% for the monofunctional complexes **3-2F** and **4-F**, respectively.

The B−F bond elongation for the bidentate Lewis acid complexes indicates a significant interaction with the adjacent tin center, which leads to weakening of the B−F bond, and is further reflected in the structural distortions as seen from the lower tetrahedral character in comparison to the mono-

(36) (a) Toyota, S.; Oki, M. *Bull. Chem. Soc. Jpn.* **1992**, *65*, 1832−1840. (b) For a review that discusses the tetrahedral character of boron compounds and an alternative analysis, see: Höpfl, H. *J. Organomet. Chem.* **1999**, *581*, 129−149.

functional borate complexes. However, the B−F_{br} bond distances for all compounds are considerably shorter than the B−F distances in those complexes, in which fluoride is equidistant to both boron Lewis acid sites or almost so. Examples include Herberich's[30] diborylcobaltocenium complex Co[C_5H_4(B*i*Pr_2)]$_2$(μ-F) with 1.641(4) Å and Gabbaï's[15] naphthalenediborane system **A** with 1.585(5) and 1.633(5) Å.

Tin Environment. All complexes adopt monomeric structures in the solid state. In particular, **1-3F** and **2-2F** do not show any significant intermolecular Sn···F interactions. The latter is unusual in that triorganotin fluorides typically aggregate to form polymeric structures through bridging fluorines.[37] In rare cases, dimeric species are observed with a fluorine atom in the bridging position,[38] and monomeric structures are only realized with exceptionally bulky substituents on tin, as for example, in Mes_3SnF[39,40] (Mes = 2,4,6-$C_6H_2Me_3$) and ($(SiMe_3)_3C$)Ph_2SnF.[41] In our complexes, the Sn−F_t (F_t = terminal fluorine) bond distances are slightly longer than those reported for typical monomeric triorganotin fluorides. For example, the Sn−F bond distances for **1-3F** and **2-2F** amount to 2.0095(13) and 2.013(4) Å, respectively, while for monomeric Mes_3SnF,[40] distances of 1.957(4) and 1.965(4) Å were found for two independent molecules in the unit cell. The Sn−F_t elongation is attributed to the effect of binding of the bridging fluorine in the trans position at tin. A similar elongation is also observed for the terminal Sn−Cl bonds of **1-2F** and **2-F** (average of 2.433 Å; for **1** and **2**, average of 2.403 Å). However, the effect is relatively small when considering that the Sn−Cl distances for the almost symmetric bidentate Lewis acid complex [*o*-C_6H_4-($SnClMe_2$)$_2$F]$^-$ (**B**) amount to 2.532(2) and 2.608(2) Å.[6]

The distances between tin and the bridging fluoride range from 2.42 to 2.64 Å in our complexes. A literature survey of bridging Sn···F contacts in organotin fluoride aggregates shows a wide range of distances. Apart from a few reported exceptions,[37,42] polymeric triorganotin fluorides display one short and one longer Sn−F distance. For example, in Me_3-SnF the Sn−F bond distances measure 2.2 and 2.6 Å,[43] while those for the bulkier *cyclo*-Hex_3SnF amount to 2.176(6) and 2.303(10) Å.[44] Less-symmetric bridging with Sn−F distances of 1.997(3) and 2.842(3) Å was reported for the dimeric Men_3SnF (Men = menthyl).[38] Hence, the Sn···F_{br} bond distances in our complexes are within the typical range of intermolecular Sn···F_{br} bridges, consistent with the formation of B−F···Sn bridges. However, in comparison to the literature data, the terminal Sn−F_t distances in **1-3F** (2.0095-(13) Å) and **2-2F** (2.013(4) Å) are fairly short, which clearly shows that the interaction is relatively weak and that the fluoride is much more strongly bound to boron than tin. A similar situation has been observed, for example, in [(acac)$_2$-(η-C_5Me_5)Zr(μ-F)$SnMe_3Cl$] (acac = acetylacetonato), which features an asymmetric Zr−F···Sn bridge (Zr−F = 2.030-(2) Å, Sn···F_{br} = 2.462(2) Å).[45] Our observations contrast the nearly symmetric bridging between two organotin centers in [*o*-C_6H_4($SnClMe_2$)$_2$F]$^-$ (**B**) with Sn−F distances of 2.139-(3) and 2.213(3) Å.[6]

Influence of B and Sn Substituents on Fluoride Bridging. It is noteworthy that the Sn−F_{br} bond distances of **1-2F** and **1-3F** (average 2.6 Å) are significantly longer than those of **2-F** and **2-2F** (average 2.4 Å). This likely is a direct consequence of the stronger binding of fluoride to boron in the difluoroborate complexes **1-2F** and **1-3F**, which leads to shorter B−F distances as already discussed above. Another factor that may influence the Sn−F_{br} bond distance, albeit to a smaller degree, is the nature of the halide atom in trans position to the fluoride bridge. Complex **2-2F**, with a terminal fluorine atom, shows a significantly shorter Sn−F_{br} bond distance of 2.379(4) Å in comparison with that of the analogous complex **2-F** with a terminal chlorine (2.420(2) Å). This difference could be a consequence of the enhanced Lewis acidity of the tin center.[46,47] However, variations in the orientation of the B−F···Sn bridge relative to the Cp ring as discussed below are more likely to be responsible for the differences in the Sn···F_{br} distances observed for **2-F** and **2-2F**. Indeed, complexes **1-2F** and **1-3F** with Sn−F_{br} bond distances measuring 2.588(2) and 2.642(1) Å, respectively, show the reverse trend. Such a "reverse" trend has been reported previously and attributed to p_π−d_π backdonation from the halogen to the tin center.[48] Finally, interactions with the potassium counterion and crystal packing effects could also to some degree impact the Sn···F_{br} distances of the individual complexes.

Angles at Tin. All complexes display a distorted trigonal-bipyramidal geometry at tin, an arrangement that is commonly seen in pentacoordinate triorganodihalo stannates.[49] There are several methods to quantitatively assess the degree of pentacoordination. The percent pentacoordination (% TBP),[46] defined as % $TBP_{(eq)}$ = [(120° − Avg_{eq})/(120° −

(37) Beckmann, J.; Horn, D.; Jurkschat, K.; Rosche, F.; Schürmann, M.; Zachwieja, U.; Dakernieks, D.; Duthie, A.; Lim, A. E. K. *Eur. J. Inorg. Chem.* **2003**, 164−174.
(38) Beckmann, J.; Dakternieks, D.; Duthie, A. *Organometallics* **2005**, *24*, 773−776.
(39) Reuter, H.; Puff, H. *J. Organomet. Chem.* **1989**, *379*, 223−234.
(40) Beckmann, J.; Dakternieks, D.; Duthie, A.; Tiekink, E. R. T. *J. Organomet. Chem.* **2002**, *648*, 204−208.
(41) Al-Juaid, S. S.; Dhaher, S. M.; Eaborn, C.; Hitchcock, P. B.; Smith, J. D. *J. Organomet. Chem.* **1987**, *325*, 117−127.
(42) Tudela, D.; Gutiérrez-Puebla, E.; Monge, A. *J. Chem. Soc., Dalton Trans.* **1992**, 1069−1071.
(43) Clark, H. C.; O'Brien, R. J.; Trotter, J. *J. Chem. Soc.* **1964**, 2332−2336.
(44) Tudela, D.; Fernández, R.; Belsky, V. K.; Zavodnik, V. E. *J. Chem. Soc., Dalton Trans.* **1996**, 2123−2126.
(45) Murphy, E. F.; Yu, P.; Dietrich, S.; Roesky, H. W.; Parisini, E.; Noltemeyer, M. *J. Chem. Soc., Dalton Trans.* **1996**, 1983−1987.
(46) Tamao, K.; Hayashi, T.; Ito, Y.; Shiro, M. *Organometallics* **1992**, *11*, 2099−2114.
(47) (a) Dostal, S.; Stoudt, S. J.; Fanwick, P.; Sereatan, W. F.; Kahr, B.; Jackson, J. E. *Organometallics* **1993**, *12*, 2284−2291. (b) Bares, J.; Novák, P.; Nádvorník, M.; Jambor, R.; Lébl, T.; Cisarová, I.; Ruzicka, A.; Holecek, J. *Organometallics* **2004**, *23*, 2967−2971. (c) Varga, R. A.; Rotar, A.; Schürmann, M.; Jurkschat, K.; Silvestru, C. *Eur. J. Inorg. Chem.* **2006**, 1475−1486.
(48) (a) Kolb, U.; Dräger, M. *Organometallics* **1991**, *10*, 2737−2742. (b) Bajue, S. A.; Bramwell, F. B.; Charles, M.; Cervantes-Lee, F.; Pannell, K. *Inorg. Chim. Acta* **1992**, *197*, 83−87.
(49) (a) Sau, A. C.; Carpino, L. A.; Holmes, R. R. *J. Organomet. Chem.* **1980**, *197*, 181−197. (b) Colton, R.; Dakternieks, D. *Inorg. Chim. Acta* **1988**, *148*, 31−36. (c) Gingras, M.; Chan, T. H.; Harpp, D. N. *J. Org. Chem.* **1990**, *55*, 2078−2090. (d) Kolb, U.; Beuter, M.; Dräger, M. *Inorg. Chem.* **1994**, *33*, 4522−4530. (e) Rippstein, R.; Kickelbick, G.; Schubert, U. *Inorg. Chim. Acta* **1999**, *290*, 100−104.

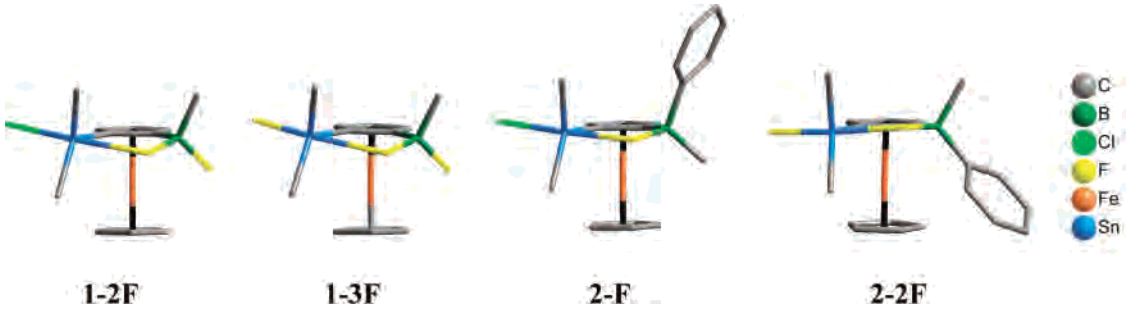

Figure 4. Illustration of the orientation of the B−F···Sn bridges relative to the Cp planes.

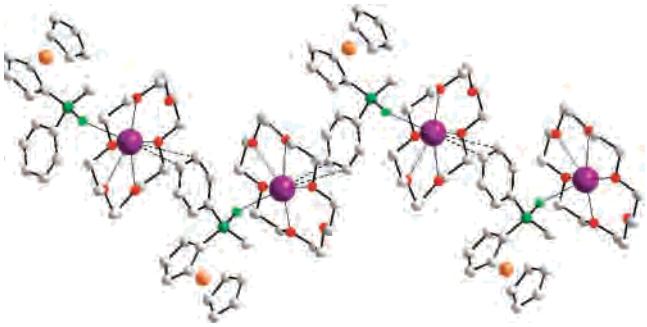

Figure 5. Extended Structure of **4-F**.

Table 2. Geometric Parameters Used to Evaluate the Trigonal-Bipyramidal Character at Tin[a]

	1-2F	1-3F	2-F	2-2F	1	2
$\Sigma\theta_{eq}$	353.5	353.1	355.2	354.3	350.6	351.9
Avg_{eq}	117.8	117.7	118.4	118.1	116.8	117.3
$\Sigma\theta_{ax}$	295.8	297.1	291.9	293.8	300.9	298.7
Avg_{ax}	98.6	99.0	97.3	97.9	100.3	99.6
% $TBP_{(eq)}$	79.4	78.2	85.0	81.9	70.2	74.3
$\Sigma\theta_{eq} - \Sigma\theta_{ax}$	57.7	55.6	63.4	60.5	49.7	53.2

[a] $\Sigma\theta_{eq}$ is the sum of the equatorial-to-equatorial angles, $\Sigma\theta_{ax}$ is the sum of the equatorial-to-axial angles, Avg_{eq} is the average of the equatorial-to-equatorial angles, and Avg_{ax} is the average of the equatorial-to-axial angles. % $TBP_{(eq)} = [(120° - Avg_{eq})/(120° - 109.5°)] \times 100\%$.[46]

109.5°)] × 100%, where Avg_{eq} is the average of the equatorial-to-equatorial angles, the difference between the sum of the equatorial-to-equatorial and the sum of the equatorial-to-axial angles ($\Sigma\theta_{eq} - \Sigma\theta_{ax}$) and the tin atom displacement from the center of the trigonal pyramid[6] were chosen as probes (Table 2). The % $TBP_{(eq)}$ for complexes **1-2F** and **1-3F** is similar and averages 79%, while the % $TBP_{(eq)}$ found for **2-F** and **2-2F** averages 83%. This slight increase reflects the stronger interaction of F_{br} in **2-F** and **2-2F** as discussed above. A similar trend is evident from the $\Sigma\theta_{eq} - \Sigma\theta_{ax}$ values, which for complexes **1-2F** and **1-3F** average 57° and for **2-F** and **2-2F** average 62° (for ideal tetrahedral geometry $\Sigma\theta_{eq} - \Sigma\theta_{ax} = 0°$; for ideal trigonal-bipyramidal geometry $\Sigma\theta_{eq} - \Sigma\theta_{ax} = 90°$). Finally, the Sn-(1) displacement in the direction of the substituent X (X = F, Cl) is 0.3141 and 0.3289 Å for **1-2F** and **1-3F**, respectively, relative to the equatorial plane defined by C(1), C(12), and C(13). Considerably smaller displacements of 0.2672 and 0.2905 Å are observed for **2-F** and **2-2F**.

We have previously shown that the tin centers in **1** and **2** also assume pseudo-trigonal-bipyramidal geometry due to the weak intramolecular interaction of tin with a chlorine and a phenyl substituent, respectively, attached to tricoordinate boron.[26] However, for the free acids **1** and **2**, this interaction results in significantly lower % TBP values of only 70.2 and 74.3%, respectively. Also, for **1** and **2**, $\Sigma\theta_{eq} - \Sigma\theta_{ax}$ is smaller with 49.7° and 53.2°, respectively, and the Sn atom displacement of 0.3810 Å for **1** and 0.3523 Å for **2** is larger. We conclude that interactions of tin with the substituents of tricoordinate boron are far less pronounced than those with fluoride in the fluoroborate complexes described here.

Orientation of the B−F···Sn Bridge Relative to the Cp Ring. The torsion angle between the B−F vector and the Cp ring (defined by B(1)−F_{br} and C(1)−C(2)) of 1.8° for **2-2F** is surprisingly different from those for the other three complexes (**1-2F** 17.9°, **1-3F** 16.4°, **2-F** 13.7°) as illustrated in Figure 4. This indicates that differences in the orientation of the boron substituents relative to the Cp plane play an important role. For **2-2F**, positioning of the Ph group below the Cp ring allows for a conformation in which the Ph group shows π interactions with the unsubstituted Cp ring. In contrast, the Me group in **2-F** avoids steric interactions with the free Cp ring through slight rotation about the Cp−B bond.[50] As a likely consequence, the Sn···F_{br} distance in **2-2F** is shorter than that in **2-F** despite a similar B−F distance for both compounds.

Interaction of K^+ with Halide Substituents. All four bidentate Lewis acid complexes show interactions of the halide substituent(s) on tin or boron with the $[K(18\text{-crown-}6)THF]^+$ counterions. In **2-F** and **2-2F**, the K^+ ion is bound to six 18-crown-6 oxygen atoms, one THF oxygen, and a terminal halide substituent on tin giving rise to octacoordinate potassium. The K(1)···Cl(1) and K(1)···F(2) contacts of 3.0250(11) and 2.579(4) Å, respectively, are considerably shorter than those found in the salt structures of KCl and KF (3.15 Å for KCl and 2.67 Å for KF).[51] The situation is rather different for **1-2F** and **1-3F**, in which the countercation simultaneously interacts with both boron-bound fluorine atoms, giving rise to nonacoordinate potassium.[52] Interest-

(50) There are no significant differences in the chemical shifts observed in solution that would correspond to the observed torsion angles measured in the solid state; the latter is in agreement with the presence of both possible B-chiral enantiomers in solution.

(51) Cotton, F. A.; Murillo, C. A.; Bochmann, M. *Advanced Inorganic Chemistry*, 6th ed.; Wiley-Interscience: New York, 1999.

(52) Examples of the coordination of fluoroborates to $[K(18\text{-crown-}6)]^+$ via multiple fluorine atoms: (a) Groux, L. F.; Weiss, T.; Reddy, D. N.; Chase, P. A.; Piers, W. E.; Ziegler, T.; Parvez, M.; Benet-Buchholz, J. *J. Am. Chem. Soc.* **2005**, *127*, 1854−1869. (b) Fei, Z.; Zhao, D.; Geldbach, T. J.; Scopelliti, R.; Dyson, P. J. *Eur. J. Inorg. Chem.* **2005**, 860−865.

Table 3. Comparison of NMR Data for **1-2F**, **1-3F**, **2-F**, **2-2F**, **3-2F**, and **4-F** in CD_3CN at 25 °C

	isomer[a]	$\delta(^{11}B)$ ($w_{1/2}$)	$J(^{11}B, ^{19}F)$	$\delta(^{119}Sn)$	$J(^{119}Sn, ^{19}F)$	$\delta(^{19}F)$	$J(^{19}F, ^{19}F)$
1-2F		10.5 (200)		42.5 (dd)	154 $F_{(I)}$	−133.3 (br)	
					99 $F_{(II)}$	−134.4 (br)	
1-3F		9.9 (230)		46.2 (ddd)	2064 $F_{(t)}$	−189.3 (pst)	19.3
					152 $F_{(I)}$	−133.7 (br)	
					93 $F_{(II)}$	−135.3 (br)	
2-F	A	5.9 (300)		27.7 (d)	344	−171 (br)	
	B	5.9 (300)		25.7 (d)	365	−168 (br)	
2-2F	A	6.3 (190)		30.8 (dd)	2038 $F_{(t)}$	−184.2 (d pst)	51.7
					342 $F_{(br)}$	−171.6 (br)	
	B	6.3 (190)		26.6 (dd)	2046 $F_{(t)}$	−183.5 (d pst)	51.7
					372 $F_{(br)}$	−169.8 (br)	
3-2F		8.1 (160)	76 (t)			−142.4 (q, 76)	
4-F		2.4 (140)	71 (d)			−189.0 (q, 71)	

[a] The isomer designations A and B are arbitrary and have not been correlated with the actual structures.

ingly, the K−F(1) (bridging fluorine) bond distance for both complexes (average 2.853 Å) is significantly longer than the average K−F(2) distance of 2.746 Å to the terminal fluorine. Also noteworthy is the significantly longer bond distance (weaker interaction) of potassium to THF in **1-2F** and **1-3F** with K(1)···O(7) averaging 2.869 Å compared with an average of 2.783 Å for **2-F** and **2-2F**.[53] Moreover, the THF molecule in **1-2F** is disordered over two positions, only one of which allows for bonding to potassium. The weaker binding of THF is most likely related to the simultaneous coordination of potassium to two fluorine atoms in **1-2F** and **1-3F**.

Complexes **3-2F** and **4-F** crystallize without THF, and **3-2F** contains a cocrystallized water molecule in the lattice, which is not coordinated to K but hydrogen bonded to one fluorine atom of each of the two independent main molecules. For **3-2F**, unusually short K−F bond distances of K(1)−F(2) = 2.6449(18) Å and K(1)−F(1) = 2.8931(17) Å are found instead. Moreover, the K ion displacement from the plane defined by O(1)−O(6) toward the fluoride substituents measures 0.8816 Å, which is greatly increased compared with those of complexes **1-2F** and **1-3F** with displacements measuring 0.5441 and 0.4809 Å, respectively. Complex **4-F** also displays an unusual coordination environment for K^+ with short contacts to the para and meta carbon atoms of the phenyl ring of an adjacent molecule ($K\cdots C_p$ = 3.373 Å and $K\cdots C_m$ = 3.490 Å), which effectively leads to the formation of a polymeric chain in the solid state, as illustrated in Figure 5.[54]

Solution Structures. The presence of NMR-active tin, boron, and fluorine atoms offers a convenient spectroscopic handle for further examination of the extent of bridging-fluoride interactions in solution. A summary of ^{119}Sn, ^{19}F, and ^{11}B NMR data is presented in Table 3. Two sets of signals are observed for the two diastereomers of **2-F** and **2-2F** in all spectra, except for the ^{11}B NMR spectra, where the broad nature of the resonances does not allow the resolution of individual signals for the isomers. We have previously observed a similar behavior for complexes of compound **2** with pyridine derivatives as neutral nucleophiles.[27] Integration of the ^1H NMR spectra of **2-F** and **2-2F** indicates that the diastereomers exist in a 1:1 ratio in solution.[55]

Boron NMR Data. The ^{11}B NMR signals range from 9.9 to 10.5 ppm for the compounds that feature a $BMeF_2^-$ group (**1-2F** and **1-3F**) and from 5.9 to 6.3 ppm for those with a $BMePhF^-$ group on ferrocene (**2-F** and **2-2F**). These values are consistent with tetracoordinated fluoroborate species[56] but reveal a distinct downfield shift relative to the monofunctional complexes (**3-2F**, 8.1 ppm; **4-F**, 2.4 ppm). Compared with symmetrically fluorine-bridged boron-based bidentate Lewis acids,[15,30,57] however, this downfield shift is small.

Tin NMR Data. The ^{119}Sn NMR spectra feature one signal for complexes **1-2F** and **1-3F** (Figure 6) but two separate signals for the different diastereomers of complexes **2-F** and **2-2F** (Figure 7). A relatively large upfield shift of the ^{119}Sn NMR resonances from 90 ppm for the free acid **1** to 42 ppm for **1-2F** and from 102 ppm for **2** to 27.7/25.7 ppm for the two diastereomers of **2-F** suggests that the fluoride is indeed coordinating to tin. Similar chemical shifts are also observed for the fully fluorinated complexes **1-3F** and **2-2F**.

An important finding from previous studies by Jurkschat and others is that the typical coupling constant ^1J (^{119}Sn, ^{19}F) values of terminal fluorides (Sn−F_t) are about 2100 Hz, while those for bridging fluorides (Sn−$F_{br}\cdots$Sn) amount to about half of that value.[18,58,59] The presence of two diastereotopic fluorine atoms on boron in **1-2F** results in the splitting of the ^{119}Sn NMR signal into a barely resolved doublet of doublets with coupling constants of 99 and 154 Hz (Figure 6). The ^{119}Sn NMR spectrum of **1-3F** displays an eight-line

(53) Complex **1-2F** features a disordered THF molecule, which in one position shows a relatively long K(1)···O(7) bond distance of 2.919(6) Å and in the other position does not coordinate to K at all. The disordered THF molecule is located in channels along the crystallographic *a* axis. The THF molecule in complex **2-2F** is also only loosely bound and can be easily removed under vacuum as confirmed by elemental analysis.

(54) Brauer, D. J.; Bürger, H.; Hübinger, R.; Pawelke, G. *Z. Anorg. Allg. Chem.* **2001**, *627*, 679−686.

(55) Even though solution studies unequivocally show the presence of two distinct diastereomers for **2-F** and **2-2F**, only one isomer was found in the solid state.

(56) Yamaguchi, S.; Akiyama, S.; Tamao, K. *J. Am. Chem. Soc.* **2001**, *123*, 11372−11375.

(57) Williams, V. C.; Piers, W. E.; Clegg, W.; Elsegood, M. R. J.; Collins, S.; Marder, T. B. *J. Am. Chem. Soc.* **1999**, *121*, 3244−3245.

(58) Kolb, U.; Dräger, M.; Dargatz, M.; Jurkschat, K. *Organometallics* **1995**, *14*, 2827−2834.

(59) Mercier, F. A. G.; Meddour, A.; Gielen, M.; Biesemans, M.; Willem, R. *Organometallics* **1998**, *17*, 5933−5936.

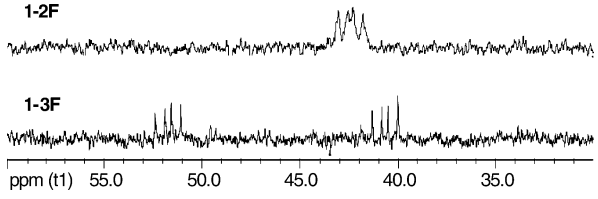

Figure 6. ^{119}Sn NMR spectra of **1-2F** and **1-3F** in CD_3CN.

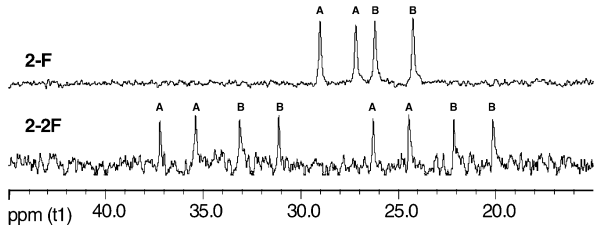

Figure 7. ^{119}Sn NMR spectra of **2-F** and **2-2F** in CD_3CN. Signals for different diastereomers are labeled as A and B.

spectral pattern consistent with an AXX′X″ spin system.[60] The large coupling constant of 2064 Hz is assigned to coupling with the terminal tin-bound fluorine, while the smaller ^{119}Sn−^{19}F coupling constants of 93 and 152 Hz are similar to those found for **1-2F** and hence are attributed to coupling with the boron-bound fluorine atoms. Similarly complex spectra are observed for **2-F** and **2-2F** due to the presence of two diastereomers (Figure 7). The two isomers of **2-F** give rise to two separate doublets with ^{119}Sn−^{19}F coupling constants of 344 and 365 Hz, respectively. The ^{119}Sn NMR spectrum of **2-2F** displays two sets of doublets of doublets with large couplings of 2038 and 2046 Hz, respectively, and smaller couplings of 342 and 372 Hz. Again, the larger splittings are due to coupling to the terminal fluorine atoms, while the smaller splittings are attributed to coupling to the bridging fluorine atoms. The most striking observation is that the coupling to the boron-bound fluorine atoms is much larger for **2-F** and **2-2F** in comparison with that for **1-2F** and **1-3F**. This indicates stronger tin−fluorine interaction and is consistent with the X-ray results discussed above. In all cases, the Sn···F_{br} coupling is considerably weaker than that in symmetric ditin complexes such as $[o\text{-}C_6H_4(SnClMe_2)_2F]^-$ (1100 Hz).[6]

Fluorine NMR Data. The ^{19}F NMR spectra of **1-2F** and **1-3F** consist of two broad signals in the range from −133 to −136 ppm for the diastereotopic boron-bound fluorine atoms with an additional pseudotriplet for **1-3F** that is upfield from the other signals at −189 ppm and shows unresolved tin satellites. This signal is assigned to the terminal tin-bound fluorine atom. The ^{19}F NMR spectra for **2-F** and **2-2F** also display two broad ^{19}F NMR signals in the range from −168 to −172 ppm, and for **2-2F**, two additional sharp doublets at −183.5 and −184.2 ppm with a ^{19}F−^{19}F coupling constant of 52 Hz and well-resolved Sn satellites are found (see Figure 9). The signal doubling in the case of **2-F** and **2-2F** is attributed to the presence of two diastereomers. The coupling constants for the tin satellites are in the range from 1950 to 2050 Hz, consistent with tin-bound terminal fluorines, and

(60) Macomber, R. S. *A Complete Introduction to Modern NMR Spectroscopy*, 1st ed.; Wiley-Interscience: New York, 1998.

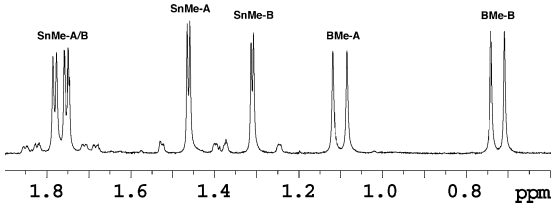

Figure 8. Methyl region of the ^{1}H NMR spectrum of **2-F** in CD_3CN. Signals for different diastereomers are labeled as A and B.

match those derived from the ^{119}Sn NMR spectra. The ^{19}F NMR shifts of F_{br} are in the range typically also observed for fluoride anions bridging two boron centers.[30,57]

Proton NMR Data. The room-temperature ^{1}H NMR spectra of all compounds were acquired in CD_3CN and exhibit the expected resonances for 1,2-disubstituted ferrocene species.[26,27] However, somewhat broadened signals are observed, particularly toward the low-frequency end of the spectra for **1-2F** and **1-3F**. Most informative is the methyl region of the ^{1}H NMR spectra. Two Sn−Me resonances for the diastereotopic Me groups and one B−Me signal are observed for **1-2F** and **1-3F**, while compounds **2-F** and **2-2F** display two sets of each of these signals due to the presence of two diastereomers (Figure 8).

The change from tetra- to pentacoordinate tin is typically associated with an increase in the *J* (^{119}Sn) coupling constants to the ligands becoming equatorial and a decrease in the *J* (^{119}Sn) couplings to the ligands becoming axial.[58] The Sn−Me signals for **1-2F** show tin satellites with average coupling constants $J(^{117/119}\text{Sn}-^1\text{H})$ of 63 and 68 Hz, while those for **1-3F** are slightly larger with 66 and 69 Hz. These coupling constants are significantly larger than those of the precursor **1** (60/63 and 63/66 Hz). Similarly, examination of the $^{117/119}$Sn satellites for the Sn−Me groups for **2-F** and **2-2F** reveals an increase of the $J(^{117/119}\text{Sn}-^1\text{H})$ coupling constant to ca. 63/66 Hz for one of the methyl groups and to 68/72 Hz for the second methyl group, compared with 57/60 and 61/64 Hz for **2**. Thus, the ^{1}H NMR spectral data are consistent with significant Sn···F_{br}−B interactions that lead to a pseudo-trigonal bipyramidal geometry at tin. These observations further suggest that the solution structures closely resemble those determined for the solid state by X-ray crystallography.

Solvent Effects and Dynamic Processes in Solution. The ^{1}H, ^{19}F, and ^{119}Sn NMR spectra are strongly solvent, concentration, and temperature dependent. For instance, a more dilute ^{1}H NMR spectrum of **1-2F** in C_6D_6 at 25 °C shows considerably sharper peaks compared with the spectrum recorded in CD_3CN. Different solvents also impact the ^{19}F and ^{119}Sn NMR characteristics. Compound **1-3F**, for example, shows a downfield shift of the ^{119}Sn NMR signal from 46 to 75 ppm in C_6D_6 and a concurrent upfield shift for the ^{19}F NMR signal of F_t to −202 ppm (vs −189 ppm in CD_3CN). Most importantly, a decrease in the $J(^{119}\text{Sn}-^{19}\text{F}_{br})$ value from an average of 122 to 47 Hz suggests weakening of the F_{br}···Sn interaction.

Signal broadening in the ^{1}H NMR spectra indicates a dynamic process in the intermediate to fast exchange range of the ^{1}H NMR time scale, which must be related to intra-

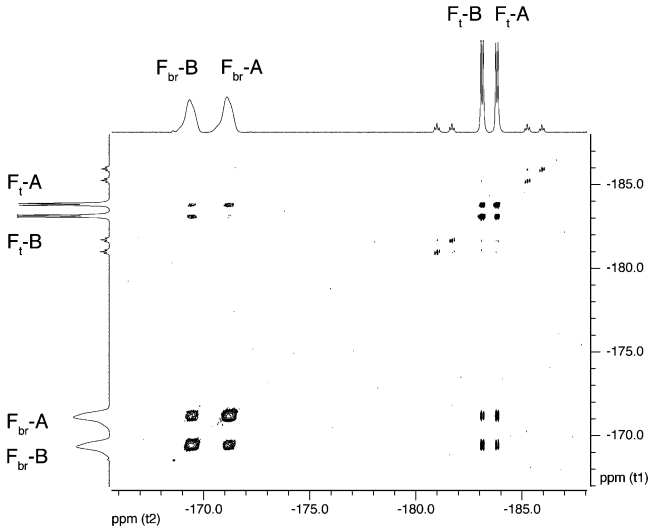

Figure 9. $^{19}F-^{19}F$ 2D-EXSY NMR spectrum of compound **2-2F** in CD_3CN; mixing time 600 ms.

and/or intermolecular exchange of fluoride ions. Complex **2-2F**, with both terminal and bridging fluorines, offers an excellent opportunity to simultaneously observe these exchange processes. We have carried out a series of room-temperature $^{19}F-^{19}F$ 2D-EXSY[61,62] (2D = two-dimensional) experiments at various mixing times ($\tau_m = 0-1300$ ms) to examine the effect of mixing time. We found the exchange processes to be virtually undetected at mixing times smaller than 300 ms. The intensity matrices obtained by integration of the cross-peaks (off-diagonal peaks) at 300, 600, and 1300 ms together with intensities of the diagonal peaks obtained at 0 ms are provided in the Supporting Information. A representative plot of the EXSY spectrum using a mixing time of 600 ms is shown in Figure 9.

Examination of the rate matrices reveals that at mixing times greater than 300 ms the highest (fastest) exchange rates are those for the intramolecular fluoride exchange and for the intermolecular cross exchange between the terminal and bridging fluorines, respectively, of different isomers. For instance, at $\tau_m = 600$ ms average rates of 0.33 s^{-1} for the exchange of F_{br} with F_t were determined, and the rate for exchange of F_t-A with F_t-B (0.33 s^{-1}) was found to be similar to that for the exchange of $F_{br}-A$ with $F_{br}-B$ (0.29 s^{-1}). However, cross-exchange between the bridging fluorine of one isomer and the terminal fluorine of the second isomer and vice versa was found to be considerably slower (<0.1 s^{-1}). These results support a two-step mechanism where an intramolecular fluoride exchange ($F_{br} \leftrightarrow F_t$) is followed by an intermolecular exchange ($F_t \leftrightarrow F_t$; $F_{br} \leftrightarrow F_{br}$) or vice versa.

Electrochemical Studies. The presence of ferrocene as the backbone for the bidentate Lewis acid complexes can be exploited to follow the binding process and to study the electronic structure of the resulting complexes by cyclic voltammetry (CV).[12,28c,34] In CH_2Cl_2/Bu_4NPF_6 as the supporting electrolyte, reversible one-electron oxidation processes were observed for all complexes with half-wave potentials of −0.37 (**1-2F**), −0.35 (**1-3F**), −0.45 (**2-F**), and −0.50 V (**2-2F**) recorded versus the ferrocene/ferrocenium couple. The fact that the complexes are in all cases more readily oxidized than the tricoordinate ferrocenylborane precursors (**1**, +0.32 V; **2**, +0.16 V in 0.05 M α,α,α trifluorotoluene/$Bu_4N[B(C_6F_5)_4]$) is consistent with tight fluoride binding to boron, which has been shown to render boryl substituents strongly electron-donating.[12,63]

Summary and Conclusion

The heteronuclear bidentate Lewis acids **1** and **2** were found to readily form complexes with fluoride. The coordination of the anion affects both the boron and tin centers, pyramidalizing the former while imposing pseudo-trigonal-bipyramidal geometry on the latter. Solid state and solution data indicate stronger binding of the fluoride anion to the boron center and only weak to moderate interactions with the tin center. A careful comparison of the individual compounds with respect to their structural parameters from X-ray analysis and their NMR spectroscopic data, in particular an evaluation of the $^{119}Sn-^{19}F$ coupling constants, indicates relatively stronger $Sn\cdots F_{br}$ interactions for complexes **2-F** and **2-2F** in comparison to those of **1-2F** and **1-3F**. This suggests that a truly bridging situation of fluoride is favored when the Lewis acidity of boron is diminished and hence more comparable to the strength of the organotin moiety. Facile fluorine exchange processes were detected by $^{19}F-^{19}F$ 2D-EXSY spectroscopy. Both intramolecular exchange between bridging and terminal fluorine atoms of the same molecule and intermolecular exchange processes were observed. Intermolecular exchange was confirmed by the observation of cross-peaks between the two different boron-chiral diastereomers of compound **2-2F**. Finally, the observation of reversible redox processes for all complexes by CV suggests that oxidation of the central iron atom may be exploited to further strengthen the fluoride binding through the formation of zwitterionic ferrocenium−borate complexes.[12,16,28c,64]

Experimental Section

Materials and General Methods. 18-crown-6 and KF were purchased from Sigma Aldrich and dried under high vacuum for 24 h. CD_3CN and C_6D_6 (>99.7%) were obtained from Cambridge Isotope Laboratories. The deuterated solvents were degassed via several freeze−pump−thaw cycles and stored over 3 Å molecular sieves. The compounds 1,2-Fc($SnMe_2Cl$)(BClMe),[25,26] 1,2-Fc($SnMe_2Cl$)(BMePh),[25,26] FcB(Cl)Me,[27] and FcB(Me)Ph[27] were prepared according to literature procedures. All reactions and manipulations were carried out under an atmosphere of prepurified

(61) Jeener, J.; Meier, B. H.; Bachmann, P.; Ernst, R. R. *J. Chem. Phys.* **1979**, *71*, 4546−4553.
(62) (a) Perrin, C. L.; Dwyer, T. J. *Chem. Rev.* **1990**, *90*, 935−967. Exchange spectroscopy (EXSY) has also been successfully applied to the elucidation of isomerization mechanisms for pentacoordinate organotin species: (b) Jurkschat, K.; Tzschach, A.; Müegge, C.; Piret-Meunier, J.; Van Meerssche, M.; Van Binst, G.; Wynants, C.; Gielen, M.; Willem, R. *Organometallics* **1988**, *7*, 593−603. (c) Wynants, C.; Van Binst, G.; Müegge, C.; Jurkschat, K.; Tzschach, A.; Pepermans, H.; Gielen, M.; Willem, R. *Organometallics* **1985**, *4*, 1906−1909.
(63) Dusemund, C.; Sandanayake, K. R. A. S.; Shinkai, S. *Chem. Commun.* **1995**, 333−334.
(64) Scheibitz, M.; Winter, R. F.; Bolte, M.; Lerner, H.-W.; Wagner, M. *Angew. Chem., Int. Ed.* **2003**, *42*, 924−927.

Table 4. Crystal Data and Structure Refinement Details of **1-2F**, **1-3F**, **2-F**, **2-2F**, **3-2F**, and **4F**

compound	**1-2F**	**1-3F**	**2-F**	**2-2F**	**3-2F**	**4F**
empirical formula	$C_{29}H_{49}BClF_2FeKO_7Sn$	$C_{29}H_{49}BF_3FeKO_7Sn$	$C_{35}H_{54}BClFFeKO_7Sn$	$C_{35}H_{54}BF_2FeKO_7Sn$	$C_{46}H_{74}B_2F_4Fe_2K_2O_{13}$	$C_{29}H_{41}BFFeKO_6$
M_r	807.61	791.13	865.68	849.23	1122.57	610.38
T, K	100(2)	150(2)	100(2)	100(2)	100(2) K	100(2) K
λ, Å	1.54178	1.54178	1.54178	1.54178	1.54178	1.54178
space group	$P2(1)/n$	$P2(1)/n$	$P2(1)/n$	$P\bar{1}$	$Pna2(1)$	$P2(1)/c$
a, Å	10.3774(6)	10.3893(4)	8.63390(10)	8.2108(8)	30.9945(3)	8.5654(3)
b, Å	17.6034(10)	17.4752(7)	29.1021(5)	14.6444(14)	8.45490(10)	15.0371(5)
c, Å	19.9566(11)	19.3552(7)	16.0961(3)	16.8450(15)	19.7835(2)	23.2270(7)
α, deg	90	90	90	84.698(7)	90	90
β, deg	103.200(2)	101.2170(10)	104.5610(10)	78.106(8)	90	98.132(2)
γ, deg	90	90	90	80.765(7)	90	90
V, Å^3	3549.3(3)	3446.9(2)	3914.48(11)	1952.6(3)	5184.37(9)	2961.53(17)
Z	4	4	4	2	4	4
ρ_{calc}, g cm^{-3}	1.511	1.525	1.469	1.444	1.438	1.369
μ(Cu Kα), mm^{-1}	11.049	10.711	10.023	9.459	6.559	5.726
final R indices $[I > 2\sigma(I)]$[a]	R1 = 0.0304	R1 = 0.0282	R1 = 0.0321	R1 = 0.0585	R1 = 0.0291	R1 = 0.0452
	wR2 = 0.0777	wR2 = 0.0722	wR2 = 0.0827	wR2 = 0.1450	wR2 = 0.0760	wR2 = 0.1201
R indices (all data)[a]	R1 = 0.0313	R1 = 0.0291	R1 = 0.0336	R1 = 0.0697	R1 = 0.0307	R1 = 0.0474
	wR2 = 0.0783	wR2 = 0.0728	wR2 = 0.0836	wR2 = 0.1553	wR2 = 0.0770	wR2 = 0.1215

[a] $R1 = \sum||F_o| - |F_c||/\sum|F_o|$; $wR2 = \{\sum[w(F_o^2 - F_c^2)^2]/\sum[w(F_o^2)^2]\}^{1/2}$.

nitrogen using either Schlenk techniques or an inert-atmosphere glovebox (MBraun Glovebox Technology). Ether solvents were distilled from Na prior to use. Hydrocarbon and chlorinated solvents were purified using a solvent purification system (Innovative Technologies; alumina/copper columns for hydrocarbon solvents), and the chlorinated solvents were subsequently degassed via several freeze−pump−thaw cycles. Elemental analyses were performed by Quantitative Technologies, Inc., Whitehouse, NJ.

All 499.9 MHz ^{1}H NMR, 125.7 MHz ^{13}C NMR, 470.36 MHz ^{19}F NMR, 186.4 MHz ^{119}Sn NMR, and 160.3 MHz ^{11}B NMR spectra were recorded on a Varian INOVA NMR spectrometer (Varian, Inc., Palo Alto, CA) equipped with a boron-free 5 mm dual broad band gradient probe (Nalorac, Varian, Inc., Martinez, CA). ^{1}H and ^{13}C NMR spectra were referenced internally to the solvent signals. ^{19}F NMR, ^{119}Sn, and ^{11}B NMR spectra were referenced externally to α,α',α''-trifluorotoluene (0.05% in C_6D_6; $\delta = -63.73$), $SnMe_4$ ($\delta = 0$), and $BF_3{\cdot}Et_2O$ ($\delta = 0$) in C_6D_6, respectively. Splittings of NMR signals are abbreviated as pst (pseudo-triplet), dpst (doublet of pseudo-triplet), and nr (not resolved).

2D proton and fluorine EXSY/NOESY[61,65] (NOESY = nuclear Overhauser effect spectrometry) measurements were obtained with the standard pulse sequence that was followed by a 90° pulse flanked by two 5 G/cm gradients for dephasing any residual transverse magnetization and suppressing potential artifacts, before the relaxation delay. Spectra were recorded in the phase-sensitive mode by employing the TPPI improvement[66] of the States−Haberkorn−Ruben Hypercomplex method.[67] Typically, 256 t1 increments of 2000 complex data points over 5.0 kHz (proton) and 11.3 kHz (fluorine) spectral widths were collected with 32 scans per t1 increment, preceded by 16 or 32 dummy scans and a relaxation delay of 2 s. Data sets were processed on a Sun Blade 100 workstation (Sun Microsystems, Inc., Palo Alto, CA) using the *VNMR* software package (Varian, Inc., Palo Alto, CA). In order to decrease t1 ridges arising from the incorrect treatment of the first data point in the discreet Fourier transform (FT) algorithm, the spectrum corresponding to the first t1 value was divided by 2 prior to FT along t1.[68] Unshifted sine bell window functions were used in both dimensions. Data sets were zero-filled in the t1 dimension yielding 1000 × 1000 final matrices. For quantitative ^{19}F NMR EXSY measurements, relaxation delays T_1 (in the range of ca. 1.8−3.7 s for different fluorine atoms) for **2-2F** have been measured by inversion recovery experiments.[69] The interpulse delay was varied from 125 ms to 16 s (8 data points). T_1 values were obtained from a nonlinear least-square fitting of an exponential curve to the peak heights. EXSY data sets were acquired using mixing times (τ_m) of 0, 20, 50, 100, 180, 300, 500, 600, 800, and 1300 ms at a temperature of 25 °C. One EXSY experiment at 1300 ms was performed with a relaxation delay longer than $(2T_1)_{max}$, which did not significantly change the computed rate constants. Cross-peak integration was performed in *MestRe-C* (version 4.9.9.3); intensities were directly used, and rates were calculated using *MestRe-C EXSYCalc*.[70]

Cyclic Voltammetry. CV measurements were carried out on a BAS CV-50W analyzer. The three-electrode system consisted of a Au disk as working electrode, a Pt wire as secondary electrode, and a Ag wire as the pseudo-reference electrode. The voltammograms of the fluoride complexes were recorded in dichloromethane containing 0.1 M Bu_4NPF_6 as the supporting electrolyte. Data were acquired with ferrocene as an internal reference and are reported relative to the ferrocene/ferrocenium couple. The voltammograms of **1** and **2** were recorded in α,α,α-trifluorotoluene containing 0.05 M $Bu_4N[B(C_6F_5)_4]$. Decamethylferrocene was used as an internal reference and the potentials are given relative to the ferrocene/ferrocenium couple (+0.63 V vs decamethylferrocene).

Crystal Structure Determinations. X-ray data were collected on a Bruker SMART APEX CCD diffractometer using Cu Kα (1.54178 Å) radiation. Crystallographic data for **1-2F**, **1-3F**, **2-F**, **2-2F**, **3-2F**, and **4-F** and details of X-ray diffraction experiments and crystal structure refinements are given in Table 4. *SADABS*[71]

(65) Macura, S.; Ernst, R. R. *Mol. Phys.* **1980**, *41*, 95−117.
(66) Redfield, A. G.; Kunz, S. D. *J. Magn. Reson.* **1975**, *19*, 250−254.
(67) States, D. J.; Haberkorn, R. A.; Ruben, D. J. *J. Magn. Reson.* **1982**, *48*, 286−292.
(68) Otting, G.; Widmer, H.; Wagner, G.; Wüthrich, K. *J. Magn. Reson.* **1986**, *66*, 187−193.
(69) Vold, R. L.; Waugh, J. S.; Klein, M. P.; Phelps, D. E. *J. Chem. Phys.* **1968**, *48*, 3831−3832.
(70) (a) Gomez, J. C. C.; Lopez, F. J. S. *MestRe-C*, version 4.9.9.3; Universidade de Santiago de Compostela: Santiago de Compostela, Spain, 2006. (b) Cobas, J. C.; Martin-Pastor, M. *Mestrelab Research*, version 4.9.9.3; Santiago de Compostela: La Coruña, Spain, 2004.
(71) Sheldrick, G. M. *SADABS, Multi-Scan Absorption Correction Program*, version 2; University of Göttingen: Göttingen, Germany, 2001.

absorption correction was applied in all cases. Structures were solved using direct methods and completed by subsequent difference Fourier syntheses and refined by full-matrix least-squares procedures on F^2. All non-hydrogen atoms were refined with anisotropic displacement coefficients. The H atoms were placed at calculated positions and were refined as riding atoms. The coordinated THF in **1-2F** is disordered. It was split over two positions and refined anisotropically. The occupancy factors for the major domain site refined to 0.525. The crystal for **3-2F** was found to be a pseudo-merohedral twin, with a ratio of 0.725:0.275(4). The two hydrogens for the cocrystallized water molecule were placed in calculated positions (0.88 Å) in the direction of a boron-bound fluorine of each of the two independent main molecules (i.e., F2 and F4). All software and source scattering factors are contained in the *SHELXTL* program package.[72] Crystallographic data for the structures of **1-2F**, **1-3F**, **2-F**, **2-2F**, **3-2F**, and **4-F** have been deposited with the Cambridge Crystallographic Data Center as supplementary publication nos. CCDC 660440−660445. Copies of the data can be obtained free of charge on application to the CCDC, 12 Union Road, Cambridge CB21EZ, U.K. (fax, (+44)1223-336-033; e-mail, deposit@ccdc.cam.ac.uk).

Treatment of Fc(BMeCl)(SnMe$_2$Cl) with 1.7 equiv KF. Synthesis of [K(18-crown-6)THF]$^+$ [Fc(BMeF)(SnMe$_2$Cl)F]$^-$ (1-2F). A solution of **1** (25.0 mg; 0.058 mmol) in 2 mL of THF was added dropwise to a mixture of KF (6.0 mg; 0.10 mmol) and 18-crown-6 (14 mg; 0.053 mmol) in 2 mL of THF while stirring. The reaction mixture was stirred at r.t. for 48 h followed by the removal of the solvent. The residue was washed first with 2 mL of hexanes and then with 2 × 1 mL of dry ether and redissolved in a 1:3 mixture of THF/ether. The mixture was kept at −36 °C for 48 h. Light orange crystals were collected and dried under vacuum. Yield: 27 mg (0.033 mmol; 66%). ^{119}Sn {^{1}H} NMR (186.4 MHz, CD_3CN, conc. 4.85 mM, 25 °C): $\delta = 42.5$ (dd, J (^{119}Sn−^{19}F$_I$) = 154 Hz, J (^{119}Sn−^{19}F$_{II}$) = 99 Hz); ^{19}F {^{1}H} NMR (470.36 MHz, CD_3CN, conc. 4.85 mM, 25 °C): $\delta = -133.3$ (br, F), −134.4 (br, F); ^{11}B {^{1}H} NMR (160.3 MHz, CD_3CN, conc. 4.85 mM, 25 °C): $\delta = 10.5$ ($w_{1/2}$ = 200 Hz); ^{1}H NMR (500 MHz, CD_3CN, conc. 4.85 mM, 25 °C): $\delta = 4.20$ (br, 1 H, Cp−H), 4.14 (br, 1 H, Cp−H), 4.10 (br, 1 H, Cp-H), 4.05 (s, 5 H, Cp−H), 3.64 (m, 4 H, THF), 3.57 (s, 24 H, 18-crown-6), 1.80 (m, 4 H, THF), 0.76 (br, ^2J ($^{117/119}$Sn, H) = 68 Hz, 3 H, Sn−Me), 0.46 (br, ^2J ($^{117/119}$Sn, H) = 63 Hz, 3 H, Sn−Me), −0.23 (pst, ^3J(^{19}F, H) = 12 Hz, 3 H, B−Me). CV (100 mV/s, vs Fc/Fc$^+$ couple): $E_{1/2} = -0.37$ V (ΔE_p = 92 mV). Anal. Calcd for $C_{29}H_{49}B_1Cl_1F_2Fe_1K_1O_7Sn_1$ (807.61): C, 43.13; H, 6.12. Found: C, 43.14; H, 5.93.

Treatment of Fc(BMeCl)(SnMe$_2$Cl) with Excess KF: Synthesis of [K(18-crown-6)THF]$^+$ [Fc(BMeF)(SnMe$_2$F)F]$^-$ (1-3F). A solution of **1** (50.0 mg; 0.11 mmol) in 2 mL of THF was added dropwise to a mixture of KF (27.7 mg; 0.48 mmol) and 18-crown-6 (32.3 mg; 0.122 mmol) in 2 mL of THF while stirring. With the use of a procedure similar to that for the preparation of **1-2F**, the product was obtained as light orange crystals. Yield: 60 mg (0.076 mmol; 65%). ^{119}Sn {^{1}H} NMR (186.4 MHz, CD_3CN, conc. 5.8 mM, 25 °C): $\delta = 46.2$ (ddd, ^1J (^{119}Sn−^{19}F$_t$) = 2064 Hz, J (^{119}Sn−^{19}F$_I$) = 152 Hz, J (^{119}Sn−^{19}F$_{II}$) = 93 Hz); ^{19}F {^{1}H} NMR (470.36 MHz, CD_3CN, conc. 5.8 mM, 25 °C): $\delta = -133.7$ (br, F), −135.3 (br, F), −189.3 (pst/m, ^2J(^{19}F−^{19}F) = 19.3 Hz, ^1J (^{19}F−$^{117/119}$Sn) = 2023 Hz, individual couplings nr, F$_t$); ^{11}B {^{1}H} NMR (160.3 MHz, CD_3CN, conc. 5.8 mM, 25 °C): $\delta = 9.9$ ($w_{1/2}$ = 230 Hz); ^{1}H NMR (500 MHz, CD_3CN, conc. 5.8 mM, 25 °C): $\delta = 4.19$ (m, 1 H, Cp−H), 4.09 (br, 1 H, Cp−H), 4.04 (s, 5 H, Cp−H), 4.03 (dd, J = 1 Hz, 2 Hz, 1 H, Cp−H), 3.64 (m, 4 H, THF), 3.57 (s, 24 H, 18-crown-6), 1.80 (m, 4 H, THF), 0.58 (m, ^2J ($^{117/119}$Sn, H) = 69 Hz, individual couplings nr, 3 H, Sn−Me), 0.29 (m, ^2J ($^{117/119}$Sn, H) = 64 Hz, individual couplings nr, 3 H, Sn−Me), −0.24 (pst, ^3J(^{19}F, H) = 12 Hz, 3 H, B−Me). CV (100 mV/s, vs Fc/Fc$^+$ couple): $E_{1/2} = -0.35$ V (ΔE_p = 105 mV). Anal. Calcd for $C_{29}H_{49}B_1F_3Fe_1K_1O_7Sn_1$ (791.15): C, 44.03; H, 6.24. Found: C, 44.10; H, 6.18.

Treatment of Fc(BMePh)(SnMe$_2$Cl) with 1.0 equiv KF: Synthesis of [K(18-crown-6)THF]$^+$ [Fc(BMePh)(SnMe$_2$Cl)F]$^-$ (2-F). A solution of **2** (104 mg; 0.221 mmol) in 2 mL of THF was added dropwise to a mixture of KF (13 mg; 0.22 mmol) and 18-crown-6 (59.5 mg; 0.225 mmol) in 2 mL of THF while stirring. With the use of a procedure similar to that for the preparation of **1-2F**, the product was obtained as light orange crystals. Yield: 135 mg (0.156 mmol; 71%). ^{119}Sn {^{1}H} NMR (186.4 MHz, CD_3CN, 25 °C): $\delta = 27.7$ (d, J (^{119}Sn−^{19}F) = 344 Hz), 25.7 (d, J (^{119}Sn−^{19}F) = 365 Hz); ^{19}F {^{1}H} NMR (470.36 MHz, CD_3CN, 25 °C): $\delta = -168$ (br), −171 (br); ^{11}B {^{1}H} NMR (160.3 MHz, CD_3CN, 25 °C): $\delta = 5.9$ ($w_{1/2}$ = 300 Hz); ^{1}H NMR (500 MHz, CD_3CN, 25 °C): $\delta = 7.49$ (d, J = 7.0 Hz, 2 H, Ph−H$_o$), 7.20 (d, J = 7.0 Hz, 2 H, Ph−H$_o$), 7.16 (pst, J = 7.5 Hz, 2 H, Ph−H$_m$), 6.98 (pst, J = 7.0 Hz, 2 H, Ph−H$_m$), 6.95 (overlapped, 1 H, Ph−H$_p$), 6.83 (t, J = 7.0 Hz, 1 H, Ph−H$_p$), 4.20 (m, 1 H, Cp−H), 4.18 (br, 2 H, Cp−H), 4.14 (overlapped, 5 H, Cp−H), 4.13 (overlapped, 1 H, Cp−H), 4.11 (br, 1 H, Cp−H), 4.10 (br, 1 H, Cp−H), 3.64 (m, 8 H, THF), 3.57 (s, 48 H, 18-crown-6), 3.56 (s, 5 H, Cp−H), 1.80 (m, 8 H, THF), 0.85 (d/dd, ^3J(^{19}F, H) = 4.5 Hz, ^2J ($^{117/119}$Sn, H) = 69/72 Hz, 3 H, Sn−Me), 0.82 (d/dd, ^3J(^{19}F, H) = 4.0 Hz, ^2J ($^{117/119}$Sn, H) = 68/71 Hz, 3 H, Sn−Me), 0.52 (d/dd, ^3J(^{19}F, H) = 3.5 Hz, ^2J ($^{117/119}$Sn, H) = 62/65 Hz, 3 H, Sn−Me), 0.37 (d/dd, ^3J(^{19}F, H) = 3.0 Hz, ^2J ($^{117/119}$Sn, H) = 63/66 Hz, 3 H, Sn−Me), 0.16 (d, ^3J (^{19}F, H) = 17 Hz, 3 H, B−Me), −0.21 (d, ^3J(^{19}F, H) = 16 Hz, 3 H, B−Me). CV (100 mV/s, vs Fc/Fc$^+$ couple): $E_{1/2} = -0.45$ V (ΔE_p = 98 mV). Anal. Calcd for $C_{35}H_{54}B_1Cl_1F_1Fe_1K_1O_7Sn_1$ (865.71): C, 48.56; H, 6.29. Found: C, 48.48; H, 6.21.

Treatment of Fc(BMePh)(SnMe$_2$Cl) with Excess KF: Synthesis of [K(18-crown-6)THF]$^+$ [Fc(BMePh)(SnMe$_2$F)F]$^-$ (2-2F). A solution of **2** (100 mg; 0.212 mmol) in 2 mL of THF was added dropwise to a mixture of KF (37 mg; 0.64 mmol) and 18-crown-6 (57.0 mg; 0.216 mmol) in 2 mL of THF while stirring. With the use of a procedure similar to that for the preparation of **1-2F**, the product was obtained as light orange crystals. Yield: 105 mg (0.135 mmol; 64%). ^{119}Sn {^{1}H} NMR (186.4 MHz, CD_3CN, 25 °C): δ = 30.8 (dd, ^1J (^{119}Sn−^{19}F$_t$) = 2038 Hz, J (^{119}Sn−^{19}F$_{br}$) = 342 Hz), 26.6 (dd, ^1J (^{119}Sn−^{19}F$_t$) = 2046 Hz, J (^{119}Sn−^{19}F$_{br}$) = 372 Hz); ^{19}F {^{1}H} NMR (470.36 MHz, CD_3CN, 25 °C): $\delta = -169.8$ (br, F$_{br}$), −171.6 (br, F$_{br}$), −183.5 (d/pst, ^1J (^{19}F−$^{119/117}$Sn) = 2049, 1951 Hz, ^2J(^{19}F−^{19}F) = 51.7 Hz, F$_t$), −184.2 (d/pst, ^1J (^{19}F−$^{119/117}$Sn) = 2040/1950 Hz, ^2J(^{19}F−^{19}F) = 51.7 Hz, F$_t$); ^{11}B {^{1}H} NMR (160.3 MHz, CD_3CN, 25 °C): $\delta = 6.3$ ($w_{1/2}$ = 190 Hz); ^{1}H NMR (500 MHz, CD_3CN, 25 °C): $\delta = 7.49$ (d, J = 6.5 Hz, 2 H, Ph−H$_o$), 7.21 (d, J = 6.5 Hz, 2 H, Ph−H$_o$), 7.16 (pst, J = 7.5 Hz, 2 H, Ph−H$_m$), 6.97 (pst, J = 7.5 Hz, 2 H, Ph−H$_m$), 6.96 (overlapped, 1 H, Ph−H$_p$), 6.82 (t, J = 7.5 Hz, 1 H, Ph−H$_p$), 4.19 (m, 1 H, Cp−H), 4.15 (overlapped, 2 H, Cp−H), 4.15 (overlapped, 5 H, Cp−H), 4.10 (br, 1 H, Cp−H), 4.02 (br, 1 H, Cp−H), 3.99 (br, 1 H, Cp−H), 3.64 (m, 8 H, THF), 3.57 (s, 48 H, 18-crown-6), 3.54 (s, 5 H, Cp−H), 1.80 (m, 8 H, THF), 0.65 (pst/dpst, ^3J(^{19}F, H) = 4.0 Hz, ^2J ($^{117/119}$Sn, H) = 69/72 Hz, 3 H, Sn−Me), 0.62 (pst/dpst, ^3J(^{19}F, H) = 4.0 Hz, ^2J ($^{117/119}$Sn, H) = 68/71 Hz, 3 H, Sn−Me), 0.33 (pst/dpst, ^3J(^{19}F, H) = 3.5 Hz, ^2J ($^{117/119}$Sn, H) = 63/66 Hz, 3 H, Sn−Me), 0.19 (pst/dpst, ^3J(^{19}F, H) = 3.5 Hz, ^2J

(72) Sheldrick, G. M. *SHELXTL*, version 6.14; Bruker AXS, Inc.: Madison, WI, 2004.

($^{117/119}$Sn, H) = nr, 3 H, Sn−Me), 0.14 (d, $^3J(^{19}F, H) = 16.5$ Hz, 3 H, B−Me), −0.23 (d, $^3J(^{19}F, H) = 16.5$ Hz, 3 H, B−Me). CV (100 mV/s, vs Fc/Fc^+ couple): $E_{1/2} = -0.50$ V ($\Delta E_p = 112$ mV). Anal. Calcd for $C_{31}H_{46}B_1F_2Fe_1K_1O_6Sn_1$ (777.15): C, 47.91; H, 5.97. Found: C, 47.95; H, 5.89.

Treatment of Fc(BMeCl) with Excess KF: Synthesis of $[K(18\text{-crown-6})]^+$ $[Fc(BMeF)F]^-$ (3-2F). A solution of **3** (77.0 mg; 0.313 mmol) in 2 mL of THF was added dropwise to a mixture of KF (54.0 mg; 0.93 mmol) and 18-crown-6 (82.6 mg; 0.313 mmol) in 2 mL of THF while stirring. With the use of a procedure similar to that for the preparation of **1-2F**, the product was obtained as a microcrystalline light orange solid. Yield: 100 mg (0.181 mmol; 58%). Single crystals for X-ray diffraction were obtained by the slow evaporation of a solution of the product in CH_2Cl_2/hexanes. ^{19}F {^1H} NMR (470.36 MHz, CD_3CN, 25 °C): $\delta = -142.4$ (qrt, J (^{19}F, ^{11}B = 76 Hz); ^{11}B {^1H} NMR (160.3 MHz, CD_3CN, 25 °C): $\delta = 8.1$ (t, J ($^{11}B-^{19}F$) = 76 Hz, $w_{1/2} = 160$ Hz); ^1H NMR (500 MHz, CD_3CN, 25 °C): $\delta = 3.96$ (s, 5 H, Cp−H), 3.88 (overlapped, 4 H, Cp−H), 3.57 (s, 24 H, 18-crown-6), −0.28 (pst, $^3J(^{19}F, H) = 11$ Hz, 3 H, B−Me).

Treatment of Fc(BMePh) with Excess KF: Synthesis of $[K(18\text{-crown-6})]^+$ $[Fc(BMePh)F]^-$ (4-F). A solution of **4** (14.7 mg; 0.051 mmol) in 2 mL of THF was added dropwise to a mixture of KF (4.3 mg; 0.074 mmol) and 18-crown-6 (16.4 mg; 0.061 mmol) in 2 mL of THF while stirring. With the use of a procedure similar to that for the preparation of **1-2F**, the product was obtained as light orange crystals. Yield: 16 mg (0.026 mmol; 51%). ^{19}F {^1H} NMR (470.36 MHz, CD_3CN, 25 °C): $\delta = -189.0$ (qrt, J ($^{11}B-^{19}F$ = 71 Hz); ^{11}B {^1H} NMR (160.3 MHz, CD_3CN, 25 °C): $\delta = 2.4$ (d, ^1J ($^{11}B-^{19}F$) = 71 Hz, $w_{1/2} = 140$ Hz); ^1H NMR (500 MHz, CD_3CN, 25 °C): $\delta = 7.38$ (d, $J = 7.0$ Hz, 2 H, Ph−H_o), 7.01 (pst, $J = 7.5$ Hz, 2 H, Ph−H_m), 6.83 (t, $J = 7.0$ Hz, 1 H, Ph−H_p), 3.92 (s, 5 H, Cp−H), 3.83 (overlapped, 4 H, Cp−H), 3.57 (s, 24 H, 18-crown-6), −0.04 (pst, $^3J(^{19}F, H) = 14$ Hz, 3 H, B−Me).

Acknowledgment. Acknowledgment is made to the donors of the Petroleum Research Fund, administered by the American Chemical Society, and to the Rutgers University Research Council for support of this research. We thank the National Science Foundation for partial funding of an X-ray diffractometer (NSF CRIF-0443538). F.J. thanks the Alfred P. Sloan foundation for a research fellowship and the National Science foundation for a CAREER award (CHE-0346828). The authors are grateful to H. Li and Dr. P. Thilagar for acquiring CV data.

Supporting Information Available: ORTEP plot of the second independent molecule of **3-2F**; ^{119}Sn NMR spectra of **1-2F** and **1-3F** in C_6D_6; intensity and rate matrices for EXSY experiments; CIF files. This material is available free of charge via the Internet at http://pubs.acs.org.

IC7013754